BODIPY-Based Semiconducting Materials for Organic Bulk Heterojunction Photovoltaics and Thin-Film Transistors

Dongil Ho,[a] Resul Ozdemir,[b] Hyungsug Kim,[a] Taeshik Earmme,[c] Hakan Usta,*[b] and Choongik Kim*[a]

The rapid emergence of organic (opto)electronics as a promising alternative to conventional (opto)electronics has been achieved through the design and development of novel π-conjugated systems. Among various semiconducting structural platforms, 4,4-difluoro-4-bora-3a,4a-diaza-s-indacene (BODIPY) π-systems have recently attracted attention for use in organic thin-films transistors (OTFTs) and organic photovoltaics (OPVs). This Review article provides an overview of the developments in the past 10 years on the structural design and synthesis of BODIPY-based organic semiconductors and their application in OTFT/OPV devices. The findings summarized and discussed here include the most recent breakthroughs in BODIPYs with record-high charge carrier mobilities and power conversion efficiencies (PCEs). The most up-to-date design rationales and discussions providing a strong understanding of structure-property-function relationships in BODIPY-based semiconductors are presented. Thus, this review is expected to inspire new research for future materials developments/applications in this family of molecules.

Introduction

Since the 1950s, inorganic semiconductors have been explored and commercialized in an extensive range of (opto)electronic applications including electronic circuits, displays, and solar cells. Alternatively, following the discovery of conductive polymers by Heeger, MacDiarmid, and Shirakawa et al., organic (semi)conductors have also attracted great scientific and technological interest.[1] This breakthrough in 1970s has clearly revealed that organic compounds could transport electric current by proper molecular design and controlled doping, and, as a result, organic (semi)conductors have become the key components in organic (opto)electronic devices, especially in organic thin-films transistors (OTFTs) and organic photovoltaics (OPVs).[2–11] Thanks to the advancements in the past four decades in the design and development of organic semiconductors, OTFTs have emerged as an alternative technology to conventional transistors for cost-effective, large-area, printable, and flexible electronics,[12–21] and OPVs have emerged as a viable source of low-cost renewable energy with zero carbon-emission in everyday life. OPVs are also envisioned to address numerous environmental issues mainly caused by fossil fuels. An OTFT relies on the solid-state charge transport character-

istics of a π-conjugated organic semiconductor along its thin-film plane which is in contact with a gate dielectric, and its charge-transport ability is modulated by applying a gate bias. On the other hand, in an OPV device, an additional photon absorption process by the organic semiconductor is required and the solid-state charge transport occurs in the perpendicular direction to the organic semiconductor thin-film. The performance of organic semiconductors in these devices is highly influenced by the corresponding (opto)electronic/physicochemical properties and thin-film microstructure/morphology, which are all closely related to its chemical structure at the molecular level.

Regarding the continuing developments in OTFTs and OPVs, the design and synthesis of novel high-performance π-conjugated organic semiconductors is of utmost importance to advance the existing device performances/technologies and realize novel functions, and to elucidate chemical structure-property-performance relationships. For the design of organic semiconductors, realizing new building blocks with effective π-conjugation and favorable structural/electronic properties is of particular interest. In the past several decades, many structurally varied organic π-scaffolds, mainly comprised of some of the first three row elements, H, B, C, N, O, F, S, and Cl, have been designed and studied. Nonetheless, in the construction of these π-structures, boron (B) has played a very limited role, and, until very recent, there has been only a handful examples of B-containing organic semiconductors in (opto)electronics. Boron is a unique metalloid element located in Group-13 that has three valence electrons, and when it participates in molecular structures making three bonds, one of its p-orbitals remains unoccupied. Thus, most of the boron-containing molecules such as BF_3 and BH_3 have strong electron-accepting properties, and they are used as Lewis acids and catalysts in various fields of chemistry and materials science. Although boron-containing three-coordinate molecular structures are not attractive build-

[a] D. Ho, H. Kim, Prof. C. Kim
Department of Chemical and Biomolecular Engineering
Sogang University
Mapo-gu, Seoul 04107 (Republic of Korea)
E-mail: choongik@sogang.ac.kr
[b] R. Ozdemir, Prof. H. Usta
Department of Materials Science and Nanotechnology Engineering
Abdullah Gul University
Kayseri 38080 (Turkey)
E-mail: hakan.usta@agu.edu.tr
[c] Prof. T. Earmme
Department of Chemical Engineering
Hongik University
Mapo-gu, Seoul 04066 (Republic of Korea)

ing blocks for electron-transporting semiconductors since they tend to strongly trap electrons (*undesired charge localization*), boron could offer great advantages in its four-coordinate structures to construct favorable π-scaffolds. To this end, 4,4-difluoro-4-bora-3a,4a-diaza-s-indacene (BODIPY) (Figure 1) has
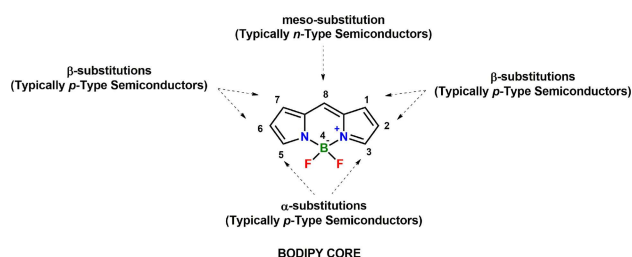
been the most attractive boron(*four-coordinate*)-containing π-electron deficient building block with favorable structural and electronic properties.

4,4-difluoro-4-bora-3a, 4a diaza-s-indacene (BODIPY) core was first discovered in 1968 by Treibs and Kreuzer.[31] Since then, numerous synthetic methods have been developed and BODIPY derivatives have been extensively studied in various applications including chemosensors, electroluminescent devices, fluorescent switches, and biochemical labelling.[32–35] Only recently, BODIPY-based small molecules, macromolecules, and polymers have emerged as promising electro-active materials in OPVs and OTFTs thanks to their strong absorbance at low energies extending to the near infrared region, low optical band gaps, high molar extinction coefficients, high thermal/photo-stability, efficient luminescence, and favorable redox properties. In addition, from a molecular design perspective, the BODIPY π-core shows good solubility in common organic solvents, energetically stabilized LUMO level, and facile synthesis/functionalization at several positions (Figure 1).[36] Its highly electron-deficient and coplanar π-core with a high dipole moment ($\mu = 3$–5 D) and good π-delocalization makes it an

Figure 1. Chemical structure of the 4,4-difluoro-4-bora-3a,4a-diaza-s-indacene (BODIPY) π-core and typical substitution positions in the synthesis of organic semiconductors.

Dongil Ho completed his bachelor's degree in chemical and biomolecular engineering in 2017 from Sogang University, South Korea. He is currently pursuing a Ph.D. degree at Sogang University under the supervision of Prof. Choongik Kim. His main scientific interests are the application of novel π-conjugated materials for organic thin-film transistors and modification of interfacial characteristics for device stability.

Resul Ozdemir graduated with a bachelor's degree in chemistry from Ankara University, Turkey in 2008, and obtained his master's degree from Abdullah Gül University in 2016. He is currently pursuing a Ph.D. degree at Abdullah Gül University under the supervision of Prof. Hakan Usta. His research interests include theoretical design and synthetic development of novel molecular and polymeric π-conjugated materials for next-generation optoelectronic devices.

Hyungsug Kim was awarded his B.S. in chemical and biomolecular engineering and electronic engineering from Sogang University in 2016. After obtaining his M.S degree under the supervision of Prof. Choongik Kim at Sogang University in 2018, he is currently working at the HBM Process Integration division of SK HYNIX in South Korea.

Taeshik Earmme obtained his B.S. and M.S. degrees in Chemical Engineering at the Seoul National University and completed his Ph D. under Prof. Sam Jenekhe at the University of Washington, on organic light-emitting diodes (OLEDs) and organic photovoltaics (OPVs) research. He then worked as an Associate Engineer at the Phillips 66 Research Center, Bartlesville (OK, USA) from 2014 to 2018. Since 2018, he has held the position of Assistant Professor in the Department of Chemical Engineering at Hongik University, South Korea.
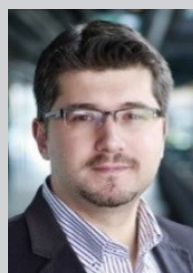
Hakan Usta obtained his Ph.D. in Chemistry from Northwestern University under the supervision of Prof. Tobin J. Marks. He then joined Polyera Corporation (IL, USA), where he held Senior Research Scientist and Project Leader positions between 2008 and 2013. He is currently an Associate Professor in the Department of Materials Science and Nanotechnology Engineering at Abdullah Gül University. He has published more than 50 research articles, 2 book chapters, and holds 13 international patents on organic (opto) electronics.

Choongik Kim completed his Ph.D. in Chemistry at Northwestern University under the supervision of Prof. Tobin J. Marks. After working as a Postdoctoral Associate with Prof. George M. Whitesides at Harvard University, he was appointed as Assistant Professor at Sogang University in 2011. He is currently an Associate Professor in the Department of Chemical and Biomolecular Engineering at Sogang University. He has published more than 80 research articles on flexible electronic devices and related optoelectronics materials.

ideal acceptor unit for the design of donor-acceptor type semiconducting architectures. We should note that although fluorine is the typical substituent on the *four-coordinate* boron center (4,4-positions) and carbon is the typical atom at 8-position, a number of different BODIPY building blocks have been realized in (opto)electronic applications with different substituents (e.g., cyano (−CN), acetylenyl (−C≡C−), and fluorene π-unit) at 4,4-positions and different atoms (e.g., nitrogen in *aza*-BODIPY) at 8-position. Although BODIPYs have very interesting structural/electronic characteristics with a great potential for further advancements in OPV and OTFT applications, a decade ago, they have rarely been studied and generally exhibited very low carrier mobilities ($\sim 10^{-5}$–10^{-3} cm^{2}V^{-1}s^{-1}),[37–45] and poor photovoltaic performances (PCEs of only 1–2%).[37,46–55] Only very recent efforts in the past five years, including some work from our research groups, have advanced the performance of BODIPY-based materials in (opto) electronics reaching carrier mobilities of ~ 0.01–0.2 cm^{2}V^{-1}s^{-1} and PCEs of ~ 6–9%. Therefore, detailed knowledge of the up-to-date results in BODIPY-based semiconductors, which is the focus of this review, and continuous research into the development of novel BODIPY-based semiconductors is of great importance to broaden the understanding of their charge transport properties and to advance the corresponding device performances.

This review intends to provide an overview of the recent progress on the design and development of BODIPY-based organic semiconductors, and their applications in OTFT and OPV devices. Since numerous comprehensive review articles have focused on the working principles of OTFT and OPV devices, no detailed attempt is made here.[56,57] This review is structured based on four main BODIPY-based semiconductor types: (1) semiconductors with a central BODIPY π-unit, (2) semiconductors with terminal BODIPY π-units, (3) annulated BODIPY semiconductors, and (4) copolymers based on BODIPY π-acceptor. At the end, we conclude with the potentials and challenges of BODIPY π-building blocks for future progress in OTFT and OPV technologies.

BODIPYs in Bulk Heterojunction Organic Photovoltaics

Inorganic solar cells are relatively mature technologies, and the power conversion efficiencies have reached 26.7% for crystalline silicon photovoltaic cells (PVs).[22] However, silicon solar cells could not be applied to flexible substrates, and they are difficult to manufacture in large sizes with low costs due to limitations in fabrication technologies. These shortcomings of silicon PVs and its inability to provide cost-effective energy solution is some of the reasons why alternative materials are still attractive for solar energy conversion systems. To this end, one of the most promising classes of materials are π-conjugated organic semiconductors that are blended in an electro-active bulk-heterojunction (BHJ) layer. BHJ-OPVs could be manufactured via very simple and cost-effective solution-based methods such as spin-coating, spray deposition, and printing.[23–30] During recent years, remarkable developments have been achieved in BHJ-

OPVs through the optimization of molecular design on the active/interfacial layers along with the morphology control and improved fabrication methods. Mostly, polymer donor-based OPVs have displayed higher power conversion efficiencies (PCEs) compared to the small molecule-based devices. However, small molecule-based semiconductors are advantageous for their simple synthesis, easy purification, versatile molecular structure, and minimal batch-to-batch variation.[58,59] These organic materials were applied as donors and acceptors in the BHJ architecture, and various building blocks have been studied throughout the years.[60–62] Among these, the BODIPY-based π-structures commonly exhibit high absorption coefficient with absorption maxima in the visible spectral region and high photoluminescence efficiency. Especially, the BODIPY π-core possesses deep HOMO level (< -5.2 eV) and efficient π-stacking in the thin-film state, making it an attractive candidate for OPV application. In this section, we summarize the recent progress (Table 1) in the past decade in BODIPY-based BHJ-OPVs focusing on four main material types and investigating the corresponding molecular design, optical-electrochemical characteristics, and device performances along with microstructural/morphological properties.

Semiconductors with a Central BODIPY π-Unit

The small molecules developed with a central BODIPY π-unit exhibit good hole transporting semiconductor behavior, and they have all been characterized as donor materials in BHJ-OPVs. The early examples of semiconductors with a central BODIPY π-unit were developed by Rousseau et al. as a series of solution processable small molecules.[46] The new molecules **1** and **2** (Figure 2) were synthesized by introducing one or two styryl units at 3,5-positions, which allowed the extension of π-conjugation and resulted in reduction of the HOMO-LUMO gap. Oligo-oxyethylene chains ensured good solubility and film-forming properties. BHJ photovoltaic devices were fabricated by using **1** or **2** as donor and PCBM as acceptor in a 1:2 donor/acceptor weight ratio. The bulk-heterojunction device configuration was realized by spin-coating chloroform solution of the blend on ITO-coated glass substrate treated with a film of PEDOT-PSS film. Both devices exhibited short-circuit current densities (J_{sc}) exceeding 4.0 mA cm^{-2}. The device based on **1** gave open-circuit voltage (V_{oc}) of 0.796 V with filling factor (FF) of 34%, which led to power conversion efficiency (PCE) of 1.17%. The cell based on **2** showed lower V_{oc} of 0.753 V, agreeing well with its higher HOMO level as compared to **1**.[80,81] This device presented an improved FF value of 44%, which suggests that the more π-extended molecular structure of **2** leads to better hole-transport performance with PCE of 1.34%. Following their original report,[46] in a separate study,[47] the same research group improved the device performance by blending **1**, **2** and PCBM in 1:1:2 weight ratio in the bulk-heterojunction layer. The device exhibited J_{sc} of 4.70 mA cm^{-2} and V_{oc} of 0.866 V with FF of 42%, which overall led to an increased PCE of 1.70%. Thus, blending dyes with complementary absorption properties led to a synergistic effect that yielded

Table 1. Photophysical and photovoltaic performance of bulk heterojunction organic photovoltaics (BHJ-OPVs) based on BODIPY derivatives.

Year	Material	λ_{max} [nm]	HOMO [eV]	LUMO [eV]	Band gap [eV]	J_{sc} [mA cm^{-2}]	V_{oc} [V]	FF [%]	PCE [%]	Ref.
2009	1[a]	572	−5.69	−3.66	2.03	4.43	0.796	34	1.17	[46]
	2[a]	646	−5.56	−3.75	1.81	4.14	0.753	44	1.34	
2009	1+2[a]	–	–	–	–	4.70	0.866	42	1.70	[47]
2010	3[a]	649	–	–	1.70	7.00	0.75	38	2.17	[63]
2011	42[b]	715	−5.22	−3.65	1.57	5.8	0.81	53	2.40	[64]
2011	43[a]	733	−4.71	−2.57	2.14	7.0	0.85	71	4.30	[65]
	44[a]	747	−4.62	−2.52	2.10	6.8	0.85	70	4.00	
2012	4[a]	580	−5.47	−3.48	1.99	8.25	0.988	39.5	3.22	[48]
	5[a]	532	−5.46	−3.40	2.06	5.22	0.914	31.7	1.51	
	6[a]	582	−5.42	−3.44	1.98	7.51	0.928	36.7	2.56	
	7[a]	534	−5.42	−3.39	2.03	6.16	0.901	33.3	1.85	
2012	45[a]	673	−4.26	−3.75	0.51	2.9	0.51	35	0.52	[49]
2012	8[a]	667	−5.46	−3.81	1.65	5.84	0.76	31	1.40	[50]
	9[a]	714	−5.32	−3.86	1.46	14.3	0.7	47	4.70	
	10[a]	724	−5.30	−3.85	1.45	5.1	0.56	30	0.90	
	11[a]	713	−5.34	−3.84	1.50	8.5	0.55	32	1.50	
2014	12[a]	737	−5.43	−4.08	1.35	5.8	0.62	35	1.26	[51]
2014	13[a]	748	−5.00	−3.59	1.41	7.00	0.68	31	1.50	[52]
	14[a]	710	−4.96	−3.42	1.54	3.59	0.43	32	0.51	
2014	15[a]	733	−5.02	−3.64	1.38	6.80	0.67	34.3	1.56	[53]
	16[a]	752	−5.06	−3.74	1.32	7.62	0.72	35.7	1.96	
	17[a]	741	−5.06	−3.73	1.33	11.28	0.74	37.5	3.13	
2014	18[a]	766	−5.14	−3.50	1.64	5.5	0.71	31	1.20	[54]
	19[a]	760	−5.02	−3.37	1.65	8.9	0.51	34	1.50	
2014	30[a]	518	−5.40	−3.79	1.61	3.09	0.65	60	1.21	[37]
	31[a]	516	−5.16	−3.82	1.34	3.90	0.62	63	1.51	
	32[a]	516	−5.14	−3.74	1.40	3.28	0.57	63	1.18	
2014	P1[a]	677	−5.30	−3.50	1.80	2.23	0.86	48	0.99	[55]
2015	46[b]	602	−5.15	−2.75	2.40	8.7	0.81	63	4.50	[66]
2015	47[b]	715	−5.22	−3.65	1.57	8.0	0.81	59	3.80	[67]
	48[b]	718	−5.16	−3.63	1.53	7.0	0.71	55	2.70	
	49[b]	729	−5.09	−3.60	1.49	5.4	0.61	52	1.70	
2015	33[a]	746	−5.01	−3.73	1.28	13.39	0.73	37.3	3.62	[68]
	34[a]	742	−5.02	−3.73	1.29	7.76	0.76	35.6	2.10	
2015	20[a]	628	−5.36	−3.81	–	-	–	–	–	[69]
	21[a]	696	−5.40	−3.81	1.59	7.64	0.73	38	2.12	
	22[a]	623	−5.15	−3.46	–	-	–	–	–	
	23[a]	601	−5.41	−3.60	–	-	–	–	–	
	24[a]	670	−5.17	−3.58	–	-	–	–	–	
2015	35[a]	641	−5.23	−3.72	1.51	10.55	0.97	46.5	4.75	[70]
	36[a]	576	−5.49	−3.69	1.80	3.49	0.99	43.5	1.51	
	37[a]	677	−5.16	−3.71	1.45	4.15	0.87	46.4	1.67	
2015	P5[a]	444	−5.16	−4.02	1.15	3.39	0.59	56.2	1.10	[71]
2016	50[b]	707	−5.13	−3.40	1.73	10.4	0.77	57.3	4.5	[72]
	51[b]	705	−5.06	−3.43	1.63	8.6	0.74	57.3	3.7	
	52[b]	753	−4.99	−3.48	1.51	8.5	0.61	51.0	2.6	
2017	25[a]	627	−4.93	−3.28	1.65	13.79	0.768	66.5	7.20	[73]
2017	26[a]	765	−5.26	−3.91	1.35	13.9	0.64	65	5.80	[74]
	27[a]	760	−5.26	−3.93	1.33	10.0	0.75	39	2.90	
2017	P2[a]	736	−5.32	−3.97	1.35	16.36	0.66	56	6.16	[38]
2017	38[a]	552	−5.24	−3.39	1.85	6.93	0.79	47.5	2.58	[75]
	39[a]	554	−5.18	−3.46	1.72	8.37	0.72	50.1	2.98	
	40[a]	550	−5.11	−3.65	1.46	11.84	0.73	53.8	4.61	
	41[a]	548	−5.02	−3.37	1.65	9.76	0.63	54.1	3.30	
2017	53[b]	762	−4.91	−3.67	1.24	4.9	0.41	55	0.8	[76]
	54[b]	777	−5.07	−3.78	1.29	6.1	0.56	63	1.6	
	55[b]	793	−5.04	−3.81	1.23	9.0	0.48	67	1.0	
	56[b]	774	−5.00	−3.74	1.26	5.6	0.52	47	1.4	
	58[b]	797	−5.13	−3.84	1.29	5.2	0.61	51	1.6	
2018	P3[a]	713	−5.40	−3.66	1.82	12.77	0.95	61	7.40	[77]
	P4[a]	780	−5.32	−3.73	1.59	14.48	0.92	66	8.79	
2018	28[a]	818	−5.39	−3.74	1.65	12.43	0.88	61	6.67	[78]
	29[a]	861	−5.36	−3.79	1.57	14.32	0.95	67	8.91	
2018	P6[a]	624	−5.45	−3.69	1.76	13.48	1.06	65	9.29	[79]

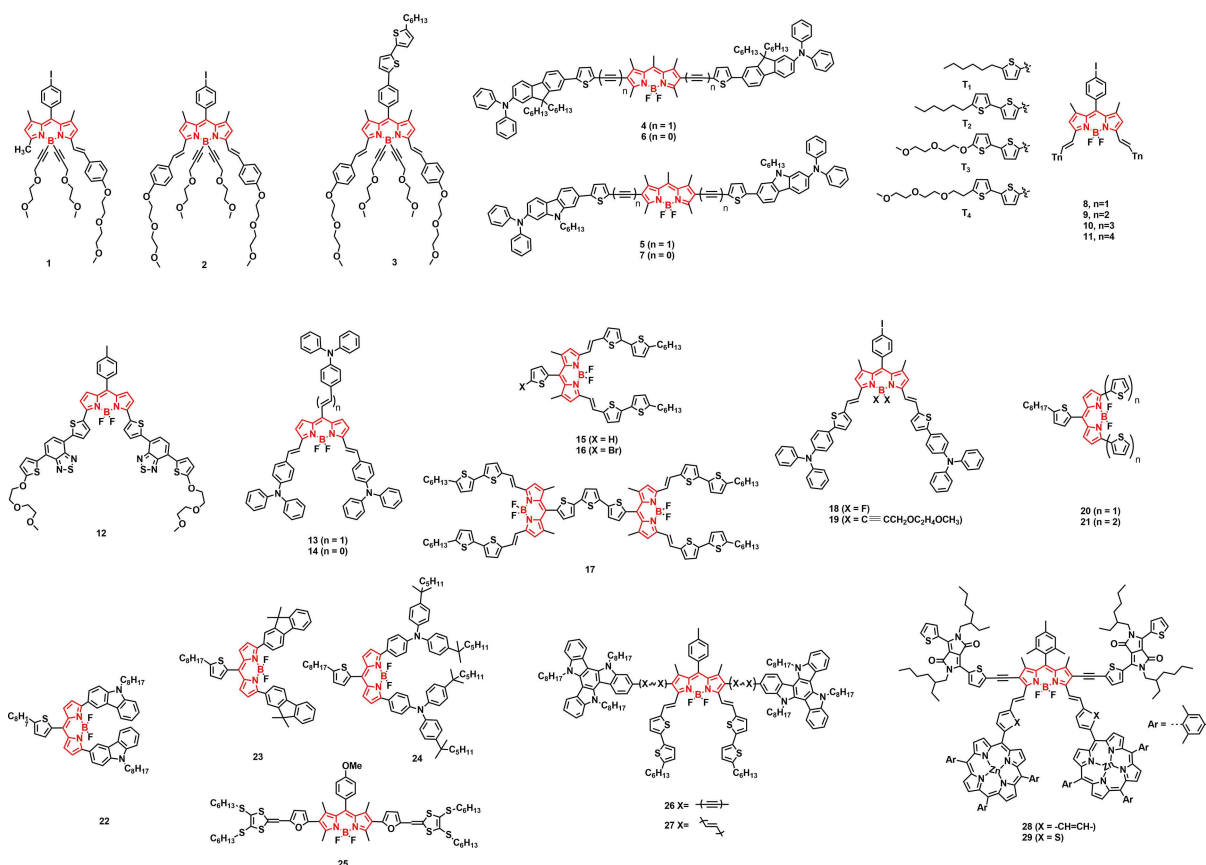[a] via solution process; [b] via vacuum deposition.

Figure 2. Chemical structures of semiconductors with a central BODIPY π-unit.

extension of photoresponse and increased power conversion efficiency.

Rousseau et al. later synthesized a new BODIPY donor (**3**), in which 5-hexyl-2,2′-bithienyl (BT) unit is attached to the *meso*-phenyl ring of **2** (Figure 2).[63] The addition of this short oligothiophene block improved the hole-transport property of **3**, as observed in other classes of *p*-type semiconductors.[82] However, the BT group had a small impact on the electronic properties of the BODIPY system due to the large twist angle associated with the thiophene-phenyl linkage and the non-coplanarity of the *meso*-phenyl ring with the dipyrromethene π-system. Cyclic voltammetry measurements showed a slight positive shift of the oxidation and reduction potentials confirming the effect of the BT unit on HOMO/LUMO energies. To fabricate BHJ cells, chloroform solution of compound **3** and PCBM (1:2 weight ratio) was spin-coated on ITO-coated glass substrate having a layer of PEDOT-PSS. The device exhibited J_{sc} of 7.00 mA cm^{-2}, V_{oc} of 0.75 V, and FF of 38%, which yielded PCE of 2.17%. Considering very similar optical and electrochemical features for **2** and **3**, the improved efficiency was not related to the increase in V_{oc} nor the light-harvesting properties; the large increase in J_{sc} suggests that the BT side chain had contributed to the hole-transport properties. This was further confirmed by fabricating ITO/Baytron/donor/Au devices and measuring the hole mobilities by space charge limited current technique. Hole mobilities of 5.10×10^{-5} cm^2 V^{-1} s^{-1} and $9.70 \times$ 10^{-5} cm^2 V^{-1} s^{-1} were measured for **2** and **3**, respectively, proving that the presence of BT chain improved the hole-transport efficiency.

Lin et al. reported small molecular BODIPY dyes incorporating conjugated substituents at the β sites (**4**–**7**) (Figure 2).[48] This was the first report applying β-substituted BODIPY small molecules in OPVs. Absorption and emission spectra of the new dyes showed the characteristic absorptions at 530–580 nm indicating elongation of the effective π-conjugation lengths. Large twist angles ($> 50°$) between BODIPY core and thiophene rings were observed for **6** and **7**, which weakens the electronic interaction between the BODIPY core and the peripheral segments. The alkyne units in **4** and **5** release the steric congestion and facilitate light harvesting. **6** and **7** experienced large Stokes shifts indicating that the excited-state molecules display a more planar conformation or a more pronounced charge-transfer state before emission. Bulk heterojunction inverted photovoltaics with the configuration of ITO/Ca/BODIPY dyes: [6,6]-phenyl C71 butyric acid methylester (PC$_{71}$BM) (1:3, w/w)/MoO$_3$/Ag were fabricated by spin-casting the active layer from chloroform solution. Different concentrations of the dyes were applied for the active layer; the resulting varied film thickness was found to play an important role in determining the electrical characteristics of the device.[88] While the open-circuit voltage (V_{oc}) value showed little dependence on the film thickness, J_{sc} and PCE values varied significantly. Both J_{sc} and FF

values increased as the film thickness decreased. This is because of increased degree of geminate and non-geminate recombinations caused by larger serial resistance in thicker films. Through optimization of the dye concentration for all small molecules, the dyes with the alkyne entity exhibited better cell performances. Especially, OPV devices with **4** showed J_{sc} of 8.25 mA cm^{-2}, V_{oc} of 0.988 V, and FF of 39.5% yielding the highest PCE of 3.22%.

Bura et al. developed a new series of thienyl-BODIPY dyes (**8–11** in Figure 2) and characterized their physical/optoelectronic properties along with their performances as active layers in both thin-film transistors and organic photovoltaics.[50] Through differential scanning calorimetry (DSC) measurements, **9** was identified as a semicrystalline material with reproducible melting and crystallization thermal transitions. The other molecules remained amorphous showing melting transitions only during the first heating ramp. Single crystal X-ray diffraction of **9** was obtained to investigate its molecular/ packing structure. **9** framework substituents displayed a coplanar structure with a nearly planar BODIPY core and a slightly curved overall structure. All four molecules exhibited fluorescence in the near-infrared region where their excitation and absorption spectra perfectly matched. The molecular energetics determined via cyclic voltammetry measurements indicate that all four molecules are suitable to be employed as electron donors with PC$_{61}$BM in BHJ devices. A low-lying HOMO level was favorable for a high V_{oc}, and the energy offset between the LUMOs of PC$_{61}$BM and donors was 0.23 V that is very close to an ideal case.[95] Charge transport performance of the current dyes were measured by applying them as a semiconductor layer in bottom-contact OTFTs, and **9** exhibited ambipolar characteristics with hole and electron mobilities of 1×10^{-3} cm^{2}V^{-1}s^{-1}, while the other molecules showed lower mobilities. The relatively high mobility value was ascribed to the short distance between neighboring molecules in its solid state. This was favored by the high propensity of the planar molecule to organize in three dimensions with strong intermolecular interactions of I⋯F and π–π-stacking. Glass/ITO/PEDOT: PSS/**8–11**:PC$_{61}$BM/Al structures were fabricated for BHJ-OPV devices, and the blended films were optimized by varying the mass ratios. Remarkably, a high J_{sc} value (14.3 mA cm^{-2}) was observed for **9** due to its optimal band gap (1.46 eV) that corresponds to the value predicted by Shockley and Queisser for a single-junction photovoltaic system[96] and the large absorption extinction coefficient. The relatively high V_{oc} value was in agreement with a deep lying HOMO level. By applying a bilayer cathode with lower **9**:PC$_{61}$BM content, slightly increased FF (47%) and PCE of 4.7% have been achieved. Relatively lower performances were achieved for **10** or **11** due to their much lower hole mobilities causing inefficient charge separation/ collection.

Mirloup et al. synthesized a new BODIPY-based molecular structure, **12**, which incorporates two thiophene-benzothiadiazole-thiophene moieties at BODIPY 3,5-positions (Figure 2).[51] The design was based on a push-pull-push architecture. In the absorption spectra of **12**, three peaks were observed; the first peak around 320 nm was due to the presence of thiophene

units overlapping with BODIPY.[97] An effective charge transfer band (CT) was observed at 537 nm due to strong electronic interaction between thiophene and benzothiadiazole units. The most intense peak ($\varepsilon = 90000$ M^{-1} cm^{-1}) appeared at 737 nm that corresponds to π–π* transition of the BODIPY unit. **12** was used as electron donor and blended with electron acceptors PC$_{61}$BM or PC$_{71}$BM to fabricate electro-active films for bulk heterojunction photovoltaics. Through the optimization of processing conditions, the devices exhibited promising PCE of 1.26%, with J_{sc}, V_{oc}, and FF values of 5.8 mA cm^{-2}, 0.62 V, and 35%, respectively.

Two near-IR absorbing BODIPY based donor molecules **13** and **14** were synthesized by Kolemen et al. (Figure 2).[52] In their previous study,[98] it has been shown that the absence of methyl groups at 1,7 positions was advantageous for extended π-conjugation and smaller dihedral angle between *meso*-phenyl units and the BODIPY core. In **13**, electron donor diphenylamino phenyl moiety was placed at the *meso* position with a styryl spacer to improve the intramolecular π-conjugation and structural flexibility. To observe the structural effects on the donor, *meso*-phenyl substituted analogue **14** was also studied. Additional diphenylamino phenyl units were attached at 3,5 positions to obtain near-IR absorptions. Both molecules showed intense and broad absorption bands in the red and near-IR region with high extinction coefficients. **13** exhibited red-shifted peak around 748 nm due to its extended π-conjugation. The HOMO/LUMO energies for **13** and **14** were measured to be −5.00/−3.59 and −4.96/−3.42 eV, respectively. Bulk heterojunction photovoltaics were fabricated with the active layer of **13**–**14**/PC$_{61}$BM, and **13** showed PCE of 1.50% with J_{sc}, V_{oc}, and FF values of 7.00 mA cm^{-2}, 0.68 V, and 31%, respectively. Structural analysis of the two small molecules was carried out, and the more twisted *meso*-substituent in **14** was found to be responsible for the decreased interaction between donor and acceptor moieties in the bulk-heterojunction layer to result in decreased device efficiency. Therefore, donor-acceptor distance could be considered as a key factor in enhancing device efficiency and, thus, as a design strategy in tuning the properties of the π-core.

Liu et al. synthesized and fully characterized three new BODIPY-based small molecular donors **15**–**17** (Figure 2).[53] Modification at the *meso*-position showed slight influence on the light-harvesting ability, energy levels, and domain sizes, but it was very effective in tuning the packing behavior in the solid state. Through two-dimensional grazing incidence X-ray diffraction (2D GIXRD) and conventional X-ray diffraction (XRD) measurements, **16**, as compared with **15**, exhibited more ordered packing behavior in the pristine film, which originated from the presence of favorable intermolecular interactions based on halogen atoms.[50] However, when PC$_{71}$BM was blended to fabricate BHJ layer, destruction of the crystalline structure occurred for both molecules. As for **17**, dimerization of the two BODIPY units expanded the π-backbone and gave the molecule a twisted structure through the "steric pairing effect" resulting in an enhanced intermolecular interaction.[99] Strong and highly ordered diffraction peaks were observed not only for the neat **17** film, but also for PC$_{71}$BM:**17** blend films.

This corresponded well with the UV-vis absorption spectra, where λ_{max} of **15** and **16** exhibited hypochromic shifts when blended with $PC_{71}BM$ while the λ_{max} of **17** remained unchanged (Figure 3). Therefore, it could be proposed that the ordered
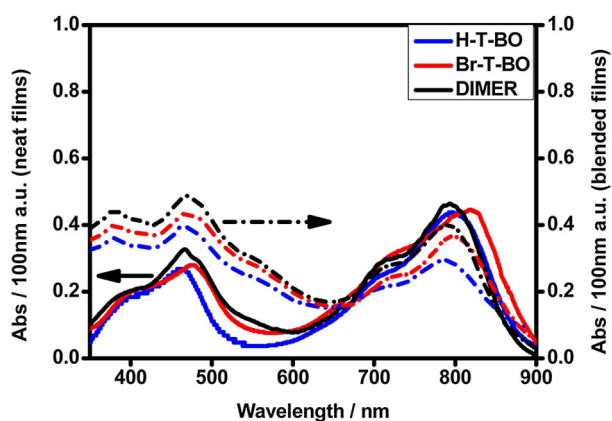

Figure 3. UV-vis absorption spectra of the three donors in the blend films (dashed lines) (1:2 for **15 (H-T-BO)**:$PC_{71}BM$ and 1:2.5 for **16(Br-T-BO)**:$PC_{71}BM$ and **17(DIMER)**:$PC_{71}BM$, w/w).[53] The absorption spectra (solid lines) for the neat films are also displayed for comparison. Copyright 2014 American Chemical Society. Reproduced with permission from ref. [53].

packing of **17** remained well both in pristine and blend films. With the fact that the packing order improved from **15** to **16** and to **17** in pristine films and even in blend film for **17**, the performance of the BHJ devices followed the same trend. **15**, **16**, and **17** exhibited J_{sc} values of 6.80, 7.62, and 11.28 mA cm^{-2}, respectively, which is followed by the PCEs of 1.56, 1.96, and 3.13%, respectively. This study demonstrated that the enhancement of intermolecular interaction and dimerization through *meso*-position clearly contributed to the J_{sc} and PCE of BODIPY-based small molecular photovoltaics.

Sutter et al. synthesized new BODIPY-based small molecules **18** and **19**, which were π-extended with vinyl-thienyl linked triphenylamine moieties (Figure 2).[54] It has been reported that the attachment of thiophene moieties on the BODIPY π-core improved the efficiency due to high carrier mobility inside the active layer.[50] Also, high open circuit voltage has been demonstrated by linking triphenylamine fragments in the 2,6-positions of the BODIPY framework.[48] Thus, the newly designed molecules were expected to exhibit increased electronic density towards thiophene sites to favor charge transfer with the electron-withdrawing BODIPY core. The molecules were blended with $PC_{71}BM$ to fabricate bulk-heterojunction solar cell devices. By optimizing the blending ratio and applying additional annealing, **19** achieved the highest PCE of 1.5% with J_{sc}, V_{oc}, and FF values of 8.9 mA cm^{-2}, 0.51 V, and 34%, respectively.

Liao et al. designed and synthesized a series of novel *meso*-thienyl BODIPY derivatives (**20–24**) with various electron-donating units (thiophene, bithiophene, carbazole, fluorene and triphenylamine) at 3,5-positions (Figure 2).[69] The derivatives exhibited good panchromatic absorption with high extinction coefficients. Especially, **21** exhibited a broad absorption band and a high extinction coefficient due to the presence of the

strongly electron-donating five-membered ring containing bithiophene moiety. This particular derivative possesses better intermolecular interactions facilitating electronic communication between donor and acceptor units in the blend layer. **21** was chosen as the electron donor material to fabricate BHJ photovoltaic devices with $PC_{61}BM$ acceptor via conventional spin-coating process. The optimized solar cell devices achieved a PCE of 2.12% with J_{sc} of 7.64 mA cm^{-2}, V_{oc} of 0.73 V, and FF of 38%.

A novel BODIPY-based small molecule, **25** with dithiafulvalene (DTF) end units, were synthesized and characterized by Rao *et al* (Figure 2).[73] DTF acted as an effective electron-donating moiety to tune the molecular optoelectronic properties and to form a stable complex with electron acceptors in photovoltaics.[118,119] A broad absorption profile was observed covering a wide spectral range of 350–780 nm extending into near-IR region. The molar extinction coefficient value (ε) at the strongest peak of 376 nm was calculated as 3.3×10^4 M^{-1}cm^{-1}, which was attributed to π-π* transition in the peripheral DTF donor unit. The HOMO and LUMO energy levels were estimated to be -4.93 and -3.28 eV, respectively, from cyclic voltammetric measurements. This indicates that the frontier molecular energy levels of the new molecule were compatible with those of popular electron acceptors for use in OPVs. A high PCE of 7.2% was measured from BHJ photovoltaic devices fabricated with solution-processed and thermally annealed **25**: $PC_{71}BM$ blend films. This was one of the highest efficiencies reported for a BODIPY-based donor. It is noteworthy that a remarkable value of 88.1% external quantum efficiency was observed at 371 nm. Furthermore, a smooth surface morphology and low RMS roughness of ~1.8 nm was measured for the annealed photoactive layer.

Bulut et al. developed and synthesized two new BODIPY-based dumbbell-shape molecules **26** and **27** with triazatruxene (TAT) moieties for OPV applications (Figure 2).[74] In the design of these molecules, self-assembling property of a previously reported BODIPY derivative, **9**,[50] was tuned by incorporating TAT end units. TAT end unit has been reported to strengthen the molecular stacking behavior.[120,121] Ethynylene and vinylene conjugated linkers were used in **26** and **27**, respectively, to link sterically-demanding TAT units to the BODIPY central core by preventing steric hindrance from weakening the electronic communication in the molecular backbone.[48] Particularly, **27** was reported to be the first example of tetra-vinylaryl substituted BODIPY-based molecule with different vinylaryl groups at 3,5 and 2,6 positions. DFT calculations confirmed the presence of highly coplanar TAT end-groups. Significant difference was observed in the film absorption spectra of **26** and **27**, suggesting distinct solid-state packing behavior for each molecule. Both small molecules were applied as electron donor in OPV devices using $PC_{71}BM$ acceptor, and **26** exhibited the highest PCE of 5.8% exceeding that of TAT-free **9**-based reference device. This result was ascribed to higher charge-carrier lifetime/mobility and much higher FF in **26**-based cells because of the presence of ethynyl-linked TAT end units.

Two novel small molecular BODIPY semiconductors **28** and **29** (Figure 2) were very recently synthesized by Bucher et al. as
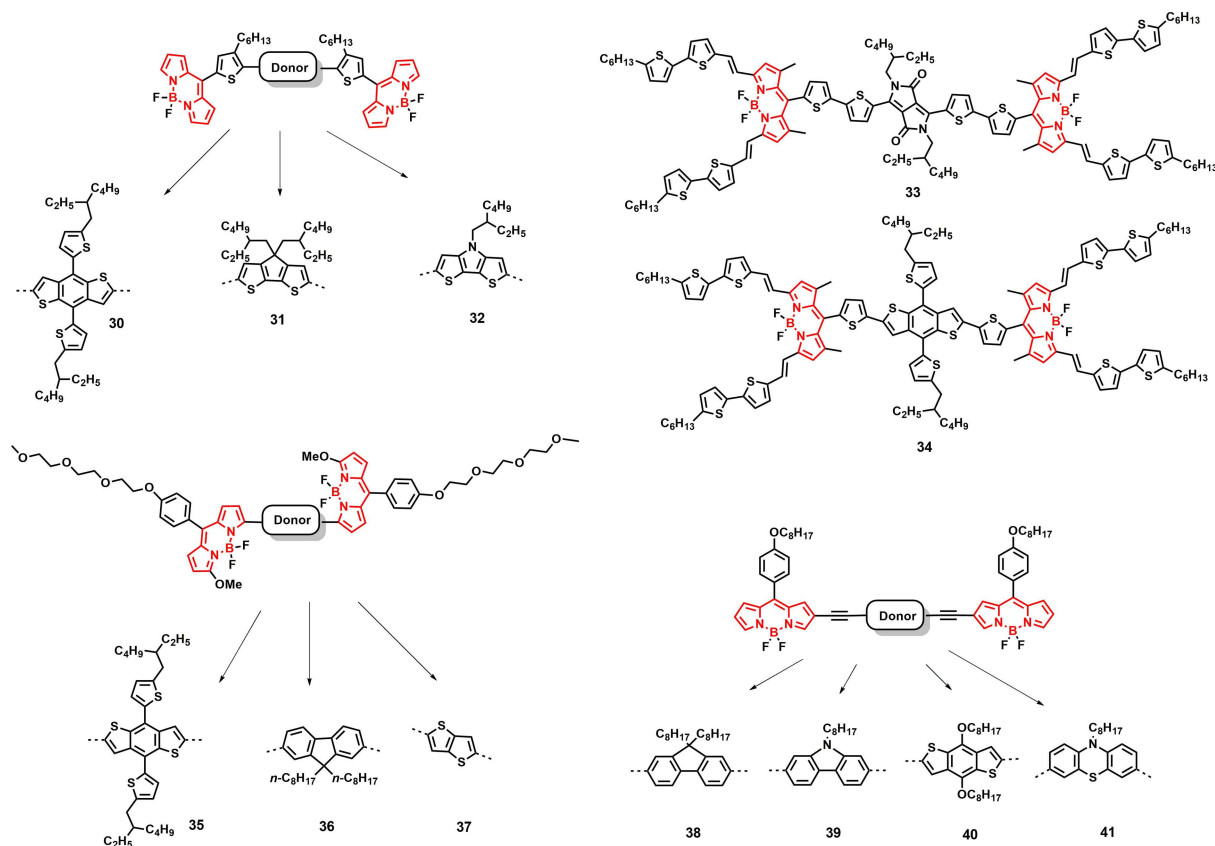
Figure 4. Chemical structures of semiconductors with terminal BODIPY π-units.

donor material for solution-processed bulk heterojunction solar cells.[78] The BODIPY core was linked to DPP units via ethynyl linkages at 2,6-positions and connected to porphyrin unit via phenyl-vinyl (**28**) and thiophene-vinyl (**29**) linkers to enable intramolecular energy transfers. In their previous report,[134] BODIPY was directly linked to porphyrin and the connection between BODIPY core and thiophene was enabled via ethynyl linker to obtain donor copolymers. **28** and **29** based thin-films showed absorbance from 400 nm to 818 nm and to 861 nm, respectively. LUMO energy levels of **28** and **29** were measured to be −3.74 eV and −3.79 eV, respectively, via cyclic voltammetry measurements. The HOMO energy levels of −5.39 eV and −5.36 eV were calculated by using LUMO and E_g values. The solar cells were fabricated within the device architecture of ITO/PEDOT:PSS/**28** and **29**:$PC_{71}BM$/PFN/Al, blend of 1:1.5 weight ratio for donor: $PC_{71}BM$. Optimized device of **28** exhibited PCEs of 3.32% with V_{oc} of 0.92 V, J_{sc} of 8.81 mA/cm^2, FF of 41%. **29** showed higher PCE of 4.73% with J_{sc} of 10.85 mA/cm^2, V_{oc} of 0.97 V, and FF of 45%. After solvent vapor annealing (SVA) in presence of CS_2, PCE significantly increased to 6.67% with V_{oc} of 0.88 V, J_{sc} of 12.43 mA/cm^2, and FF of 61% for **28**. **29**-based device showed higher performance with PCE of 8.98%, V_{oc} of 0.95 V, J_{sc} of 14.32 mA/cm^2, and FF of 67%. PL spectra revealed that the better photovoltaic performance of **29** comes from its better exciton dissociation and charge transport properties. These molecules also exhibited the energy losses of 0.63 eV and 0.50 eV, respectively. This difference originates from the lower

LUMO offset between **28** and $PC_{71}BM$ (0.31 eV) in comparison with **29** and $PC_{71}BM$ (0.36 eV). Consequently, these results are one of the highest performances in the literature for small molecular donor materials. BODIPY, DPP, and porphyrin are shown to be a very promising building block combination for further development of high-performing solar cells.

Semiconductors with Terminal BODIPY π-Units

Semiconductors developed with terminal BODIPYs are acceptor-donor-acceptor (A–D–A) type molecular systems in which BODIPYs have been employed as π-acceptors. Although most of these semiconductors have been characterized as donor materials in BHJ-OPVs, one study has demonstrated their characterization as an acceptor material. This study was conducted by Poe et al. in which they synthesized a series of A–D–A small molecules containing terminal BODIPY π-units.[37] BODIPY moieties were conjugated through their *meso*-positions using a brominated hexylthiophene linker to afford **30, 31** and **32** (Figure 4). Donor addition through α and β positions of the BODIPY core has allowed the π-conjugation to extend, resulting in red-shift of optical absorption and reduction of band gap. However, conjugation through the *meso* position yielded minimal interaction between the donor core and the terminal BODIPY units in the ground state resulting in relatively small shift in the absorption profile.[100–102] Stronger donor units

(cyclopentadithiophene and dithienopyrrole) in **31** and **32** led to red shifts in the charge transfer band resulting in low optical band gaps of 1.47 eV. Low LUMO levels of −3.7 eV and −3.9 eV were observed, respectively, which makes these molecules potential acceptors in BHJ-OPVs. Inverted bulk heterojunction photovoltaic devices were fabricated by blending the acceptor small molecules **30**, **31** and **32** with P3HT donor. PCE of 1.21% was achieved for P3HT:**30** active blend layer. Previous studies have reported the use of solvent additives to improve the efficiency of PCBM-based BHJ devices.[103–105] Since newly synthesized acceptors showed good solubility in most organic solvents, 1-chloronaphthalene was applied as a solvent additive. When 3% 1-chloronaphthalene was added, **31** yielded J_{sc}, V_{oc}, and FF values of 3.90 mA cm^{-2}, 0.62 V, and 63%, respectively, with the highest PCE of 1.51%.

Liu et al. synthesized and characterized two new BODIPY small molecules **33** and **34**, where the BODIPY end units were linked to diketopyrrolopyrrole (DPP) and 4,8-dithienyl-benzo [1,2-b:4,5-b']dithiophene (BDT) π-cores, respectively, through their meso-positions (Figure 4).[68] The absorption spectra confirmed that the central DPP moiety in **33** complements the gap between the absorption bands of two BODIPY end-units and affords enhanced absorption. The photovoltaic properties were observed by fabricating BHJ-OPV devices using PC$_{71}$BM acceptor. The devices based on **33** exhibited the best PCE of 3.62% with J_{sc}, V_{oc}, and FF values of 13.39 mA cm^{-2}, 0.73 V, and 37.3%, respectively. **34** yielded lower PCE of 2.1% with J_{sc} of 7.76 mA cm^{-2}, V_{oc} of 0.76 V, and FF of 35.6%. External quantum efficiency (EQE) and absorption spectra of the blend films were compared to investigate the contribution of the DPP π-core to the photocurrent. The DPP-containing film showed not only enhanced absorption, but also intense and sharp diffractions in XRD measurements that indicate a relatively more crystalline morphology.

Three acceptor-donor-acceptor type small molecules **35–37** were synthesized by Xiao et al., in which 8-bis(5-(2-ethylhexyl) thiophen-2-yl)benzo[1,2-b:4,5-b]dithiophene (BDTT), 9,9-dioctyl-9H-fluorene (FL), and thieno[3,2-b]thiophene (TT) donor cores were conjugated, respectively, to the α-positions of the BODIPY acceptor end-units (Figure 4).[70] The small molecules showed good solution-processability, broad and strong absorptions, and low-lying energy levels. Among these molecules, photovoltaic devices based on **35**/PC$_{71}$BM blend layer showed the highest PCE of 4.75% with J_{sc} of 10.55 mA cm^{-2}, V_{oc} of 0.97 V, and FF of 46%. Since V_{oc} depends on the energy difference between the HOMO of a donor and the LUMO of an acceptor, higher V_{oc} was obtained for the devices based on **35** and **36**, for which lower HOMO energy levels were observed. The **35**-based device yielded significantly higher J_{sc}, which was further confirmed by EQE measurements. As compared with other molecules in this study, relatively extended π-conjugation of **35** molecular backbone leads to stronger intermolecular orbital overlaps with enhanced isotropic charge transport.[116] **35**/PC$_{71}$BM blend films showed the smallest domain sizes with the optimal nanophase separation, which facilitates close contacts between **35** and PC$_{71}$BM molecules. On the other hand, **37**-based blend film displayed large globular domains,[117] which led to reduced

interfacial area between donor and acceptor units and resulted in low J_{sc}.

Liao et al. designed and synthesized four new solution processable, linear acceptor-donor-acceptor type BODIPY small molecules **38–41** by using various donor units of fluorene, carbazole, benzodithiophene, and phenothiazine (Figure 4).[75] The connections between terminal BODIPY and central donor units were made by using conjugated ethynyl units at BODIPY's 2-position, which led to the extension of molecular absorption spectra (320–700 nm) with high molar extinction coefficients (10^5 cm^{-1} M^{-1}) and strong fluorescence quenching. BHJ organic solar cells were fabricated with the device structure of ITO/ PEDOT:PSS/active layer/Ca/Al, where **38–41** were used as the donor and PC$_{71}$BM was used as the acceptor in a 1:1 weight ratio in the presence of 1% 1,8-diiodooctane (DIO) additive. **40**-based device exhibited the highest PCE of 4.65% with J_{sc} of 11.84 mA cm^{-2}, V_{oc} of 0.73 V, and FF of 53.8%. Better device performance of **40**, as compared to other molecules in this family (2.60–3.33%), originated from superior photon-electron conversion and carrier transport properties of structurally highly favorable dialkoxy-substituted benzodithiophene unit. The films of **40** showed greater intermolecular interactions, as compared with those of **38**, **39**, and **41**, which led to enhanced light absorption, increased hole mobility, and favorable surface morphology.

Annulated BODIPY Semiconductors

Annulated BODIPYs are another class of organic semiconductors which display extended π-conjugation and backbone rigidity, which together leads to high fluorescence quantum yields and strong intermolecular π–π interactions. These molecules have been characterized as donors, acceptors, and sensitizers in BHJ-OPVs and showed promising device performances. The early example of an annulated BODIPY was reported by Meiss et al. in which a transparent organic photovoltaic device was fabricated using a benzannulated BODIPY small molecule (**42**) as the donor material (Figure 5).[64] **42** was synthesized following the previously reported paper by Gresser et al.[83] This material showed an absorption peak at 773 nm, which made it applicable for devices where transparency in the visible range is as important as the absorption in the near-infrared region. The photovoltaic devices adopted an inverted p-i-n architecture in which the intrinsic absorber is sandwiched between highly conductive, doped charge transport layers. The photoactive bulk heterojunction layer was fabricated by blending **42** with C$_{60}$ and was sandwiched between an intrinsic electron transport and donor layer for better coverage of the infrared region. The device exhibited J_{sc} of 5.8 mA cm^{-2} and V_{oc} of 0.81 V with FF of 53%, which led to the highest PCE of 2.4% by modifying the illumination direction. This work demonstrated that BODIPY materials could be used for highly efficient semi-transparent organic photovoltaics.

The first example of a BODIPY molecule that worked as a sensitizer to improve the photovoltaic performance of polymeric photovoltaics has been demonstrated by Kubo et al.,
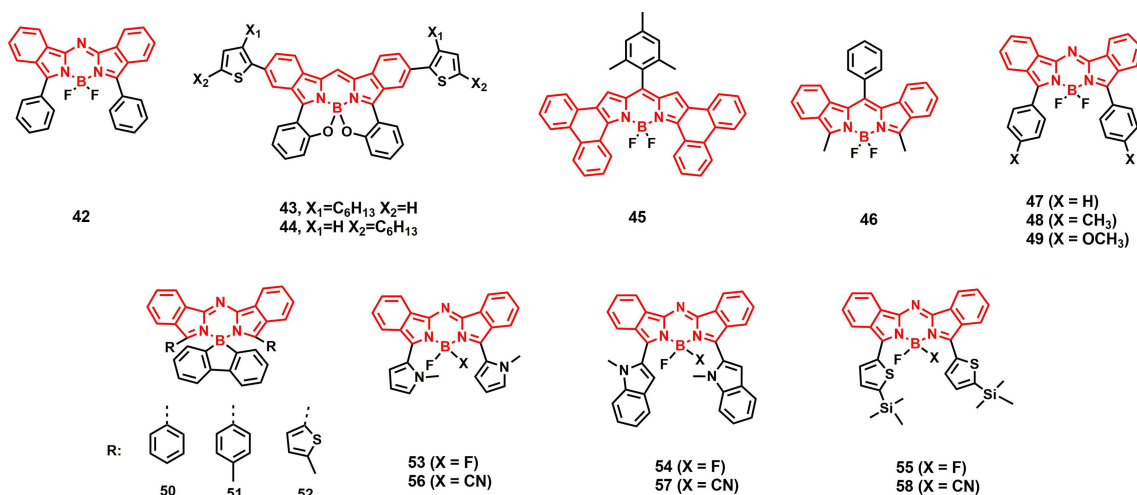
Figure 5. Chemical structures of annulated BODIPY semiconductors.

which were hexylthiophene-conjugated BODIPYs with a central benzo[1,3,2]oxazaborinine ring (**43** and **44** in Figure 5).[65] These molecules absorb near-infrared light with relatively high molecular extinction coefficients. Prior to this study, the group has developed new types of BODIPYs with benzo[1,3,2] oxazaborinine π-core relying on intramolecular B—O chelation,[84] which led to a red shift in the absorption band[85,86] yielding near-infrared absorbing dyes. Through comparison with the corresponding hexyloxy derivative, the effect of thiophene insertion on the absorption property was examined. **43** showed near-infrared light absorption with a λ_{max} value of 733 nm and the molecular extinction coefficient (ε) of $1.35 \times 10^5 \, M^{-1} cm^{-1}$, which is suitable for light-harvesting. **44** showed λ_{max} of 747 nm and ε of $1.48 \times 10^5 \, M^{-1} cm^{-1}$, where the red shift with the enhanced molecular extinction coefficient could be attributed to the degree of twists between the isoindole unit and thiophene rings in the chromophore. The newly synthesized dyes were incorporated into the electro-active layer of P3HT/IC$_{70}$BA (IC$_{70}$BA = indene-C$_{70}$ bis-adduct) in a BHJ photovoltaic cell.[87] When compared with the P3HT/IC$_{70}$BA control device, the addition of BODIPY molecules led to an increased charge carrier generation in the near-infrared region, exhibiting enhancements in the short circuit current and the PCE (Figure 6). The P3HT/IC$_{70}$BA/**43** ternary device resulted in J$_{sc}$ of 7.0 mA cm^{-2}, V$_{oc}$ of 0.85 V, FF of 71%, and PCE of 4.3%.
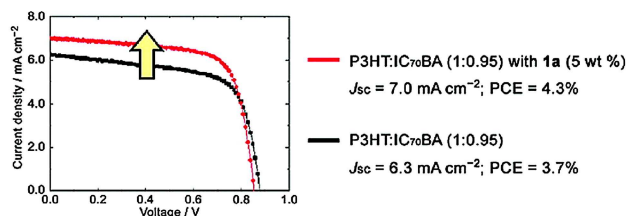
Figure 6. J–V curves for the photovoltaic devices based on P3HT:IC$_{70}$BA blend layer with and without 5 wt% **43** (shown as **1a** in the figure).[65] Copyright 2011 American Chemical Society. Reproduced with permission from ref. [65].

Hayashi et al. developed a novel aryl-fused BODIPY molecule **45** (Figure 5) and demonstrated photocurrent generation based on its n-type semiconducting property.[49] The molecule was synthesized through oxidative cyclization of β-aryl groups, and it exhibits extended π-conjugation and backbone rigidity that together leads to high fluorescence quantum yield and strong intermolecular π–π interactions. As a result, **45** demonstrated near-infrared absorption with an intense absorption maximum at 673 nm. The molecular structure of **45** is revealed by single crystal X-ray diffraction analysis, in which π-π interactions between peripheral fused-biphenyl moieties exhibited short interplanar distance of 3.48 Å. In addition, BODIPY units displayed a 1-D infinite stack, which is known to be favorable for organic semiconductors.[89–91] The electrochemical properties were also examined that indicated a low LUMO energy level of −3.75 eV. This is in the range of those of the previously reported n-type semiconductors. To verify the n-type characteristics of **45**, a p-n heterojunction photovoltaic device was fabricated employing tetrabenzoporphyrin (BP) as an electron donor.[92–94] A V$_{oc}$ of 0.51 V, J$_{sc}$ of 2.9 mA/cm^2, and FF of 35% were obtained yielding PCE of 0.52% and demonstrating the potential of BODIPY small molecules as n-type semiconductors in OPVs.

Chen et al. synthesized and investigated a novel benzannulated BODIPY **46** (Figure 5).[66] The extended π-conjugation in this molecule leads to a broader absorption in the red region of the solar spectrum (λ_{onset} ~800 nm), and π–π interactions between the fused benzene rings was expected to enhance carrier-hopping rate. **46** was used as electron donor with C$_{60}$ acceptor in a BHJ cell and demonstrated the highest performance in a bilayer architecture with a PCE of up to 4.5% (J$_{sc}$ of 8.7 mA cm^{-2}, V$_{oc}$ of 0.81 V, and FF of 63%). Furthermore, neutron reflectivity experiments were performed on the bilayer film, which revealed a 13 nm mixed layer at the donor/acceptor interface. Although each layer was deposited separately during the fabrication of these devices, spontaneous mixing of C$_{60}$ and **46** was evident. To interpret the extent of spontaneous mixing, planar-mixed heterojunction devices were fabricated, and the
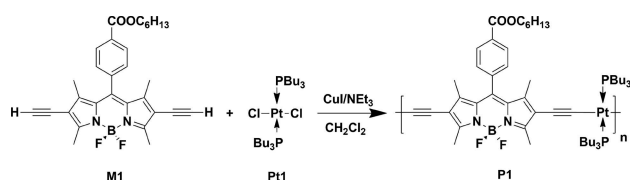
Figure 7. Synthesis and chemical structure of copolymer **P1** based on BODIPY π-acceptor.[55]

intrinsically mixed region of the bilayer device showed a **46**:C_{60} ratio of 1:3.

Three benzannulated *aza*-BODIPY molecules **47–49** (Figure 5) with different substitutions were studied in OPV devices by Kraner et al.[67] These molecules were previously studied by Gresser et al.[115] These three donors were optimized with C_{60} to fabricate bulk heterojunction photovoltaics and **47** yielded the highest PCE of 3.8% with J_{scr}, V_{ocr}, and FF values of 8.0 mA cm^{-2}, 0.81 V, and 59%, respectively. Note that this exceeded the device performance originally reported by Meiss et al.[64] When methyl/methoxy groups were added to **47**, **48**, and **49** exhibited lower PCEs of 2.7 and 1.7%, respectively. This PCE trend agreed well with the charge carrier mobilities measured by open-circuit corrected charge carrier extraction (OTRACE) method. The mobility decreased as the size of the functional group increased due to higher reorganization energy of the donor molecule and the increasing number of traps. Higher trap density was measured by impedance spectroscopy for lower performing aza-BODIPY blends. The traps originated from the bulk of the donor, which results in an increased trap density in the blend for higher donor contents. Therefore, it could be concluded that the additional side groups in the aza-BODIPYs lowered charge carrier mobilities and led to lower PCEs.

Lorenz-Rothe et al. developed new small molecular benz-*aza*-BODIPYs (**50–52**) which has fluorene groups at the boron center instead of fluorine atoms (Figure 5).[72] These semiconductors exhibited high thermal stability due to the presence of phenyl, tolyl, and methylthienyl substituents at α-positions. They also showed absorption maxima at 670–715 nm in solution and at 700–750 nm in thin-film. The hole transport characteristics of the current borafluorene compounds were found to be very similar to those with BF_2-substitutions, which is in the range of 10^{-4}–10^{-5} cm^{2}V^{-1}s^{-1}. The new molecules were employed as donor material in bulk heterojunction photovoltaics where C_{60} was used as the acceptor. **50**-based devices fabricated as a blend layer in thickness of 70 nm showed PCE of 4.4% and high EQE of 62% at 690 nm. This result is one of the highest efficiency values in the literature reported for a vacuum-processed small-molecular solar cell. These solar cell performances make borafluorene BODIPYs very promising for future developments.

Three novel benzannulated *aza*-BODIPY dyes with N-methyl pyrrole, N-methyl indole and 2-trimethylsilyl thiophene (**53–55**) substituents at α-positions were synthesized by Li *et al.* (Figure 5).[76] These dyes exhibited absorption maxima at 762–793 in solution and at 830–849 nm as thin-film with high molar extinction coefficients. So, they were used as NIR absorbers in

photovoltaics. The same research group also synthesized three additional derivatives by replacing one fluorine atom in BF_2 with a cyano group (**56–58**). These molecules also showed high extinction coefficients and outstanding absorption maxima at 774–797 nm in solution. Cyano- and fluorine-functionalized molecules exhibited different dihedral angles between the substituents at α-positions and the BODIPY π-core, which is induced by the F⋯H hydrogen bond interactions and stacking effects. Both the HOMO and LUMO energy levels are relatively more stabilized in cyano-functionalized molecules, which has a direct effect on its thermal stability. Cyclic voltammetry measurements revealed that the frontier energy levels of these semiconductors make them suitable as donor materials in photovoltaics. The bulk-heterojunction solar cells were fabricated by vacuum deposition of these molecules where C_{60} was used as the acceptor material. BHJ solar cells based on these dyes displayed PCEs of 1.4-2.6%. Further optimization of **55**-based devices revealed the best PCE value of 3.0% and V_{oc} of 0.61 V. The authors also mentioned that these molecules could be used in tandem/triple solar cells thanks to their high thermal stabilities and absorption onsets at 950 nm.

Copolymers Based on BODIPY π-Acceptor

Although BODIPY-based copolymers have been widely studied in the literature for numerous applications, until today there has been not many examples for use in BHJ-OPV devices. To this end, the only known BODIPY copolymers, **P1–P6**, are summarized here, which showed some of the best photovoltaic performances when used as the donor material in the BHJ layer. In the early study, He et al. synthesized a novel conjugated polymer, **P1**, by combining BODIPY and Pt-acetylenide building blocks (Figure 7).[55] The platinum diacetylenide moiety adopts square planar structures and serves as a structural scaffold that combine organic and organometallic chromophores to form linear conjugated polymer chains.[106–108] Moreover, the platinum complexes exhibit strong spin-orbital couplings that induce long-lived triplet exciton formation, which has been considered to be advantageous in OPVs.[109–111] **P1**:PC_{61}BM blends in different weight ratios were employed, and the highest PCE was obtained as 0.21%. It was suspected that the poor performance was due to the lack of energy level alignment and non-ohmic contact formation with the PEDOT:PSS interfacial layer. Thus, MoO_3 was thermally evaporated as the anode interfacial layer.[112–114] As a result, increased J_{scr}, V_{ocr} and FF values of 2.23 mA cm^{-2}, 0.86 V, and 48%, respectively, were measured with an improved PCE of 0.99%.

In a very recent study, a novel low band-gap D−A copolymer **P2** based on *meso*-thiophene substituted BODIPY π-acceptor **2OD-TBDY** was synthesized and characterized by Usta et al.[38] **P2** was obtained via copolymerization of **2OD-TBDY-Br$_2$** acceptor monomer with thiophene donor monomer (Figure 8). The five-membered thienyl aromatic unit at the *meso*-position minimized the dihedral angle ($\theta = 46°$) with the highly coplanar dipyrromethene π-core. This contributed to efficient π–π stacking and C−H⋯π interactions in the solid state of the

Figure 8. Synthesis and chemical structure of copolymer **P2** based on BODIPY π-acceptor.[38]

copolymer. Moreover, π-delocalization for LUMO was extended towards the *meso*-thienyl π-core, yielding favorable electronic properties. The thienyl unit at the *meso*-position effectively increased the dipole moment of the ground-state, which is expected to enhance the backbone-ordering and interchain interactions in the corresponding thin films due to strong dipolar interactions.[122] Photovoltaic characteristics of **P2** were studied by blending with $PC_{71}BM$ acceptor. Low optical band gap of 1.3 eV was observed for the copolymer, making it very attractive for optoelectronic applications.[105] Furthermore, strong interchain interactions were found through aggregation both in solution and solid state, resulting in enhanced π-coherence. Inverted BHJ devices with **P2**:$PC_{71}BM$ active layer showed PCE of 6.16%, J_{sc} of 16.36 mA cm^{-2}, V_{oc} of 0.66 V, and FF of 56% after adding 1,8-diiodooctane (DIO). The absorption spectra and film morphology of the polymer/fullerene blend with DIO was studied to clarify the enhancement effect. The absorption peak intensity had increased in the range of 800–900 nm with a slight red-shift, indicating enhanced structural ordering and interchain interactions with the addition of DIO.[123,124] Simultaneously, highly interpenetrated and small-sized domains (20–40 nm) were formed, which allowed much larger interfacial area between **P2** and $PC_{71}BM$. AFM images also

confirmed the presence of small domains with low surface roughness.

In another recent study, Bucher et al. reported two novel solution-processable, acceptor-π-donor type copolymers **P3** and **P4**, which are based on BODIPY π-acceptor and thiophene π-donor units (Figure 9).[77] The connections between donor and acceptor building blocks were enabled via ethynyl linker. **P3** displayed strong absorption profile from 500 to 800 nm with an optical bandgap of 1.74 eV. Cyclic voltammetry measurements revealed that HOMO/LUMO energy levels are −5.40 eV/ −3.66 eV for **P3** and −5.32 eV/−3.73 eV for **P4**. Widening the absorption profile (to 850 nm) and reducing the optical band gap (to 1.59 eV) were realized going from **P3** to **P4**, which originated from covalent linking of porphyrins to BODIPY's 3,5-positions. The new copolymers were employed as donor materials in bulk heterojunction photovoltaics where $PC_{71}BM$ was used as acceptor. **P3** and **P4** based optimized device showed overall PCEs of 3.03 and 3.86%, and V_{oc} values of 0.99 and 0.95 V, respectively, which was obtained in 1:2 donor/ acceptor weight ratio and by casting from dichlorobenzene solution. The difference in the open circuit voltage originated from more stabilized HOMO energy level of **P3**. After solvent vapor annealing (SVA) in DCM, the device performance

Figure 9. Chemical structures of copolymers **P3** and **P4** based on BODIPY π-acceptor.[77]
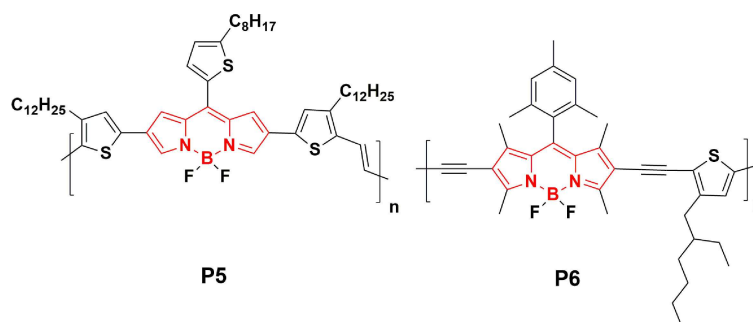
Figure 10. Chemical structures of copolymers **P5** and **P6** based on BODIPY π-acceptor.[71,79]

dramatically increased to PCE values of 7.40 % ($V_{oc}=0.95$ V, $J_{sc}=$ 12.77 mA/cm², and FF = 61 %) for **P3** and 8.79 % ($V_{oc}=0.92$ V, $J_{sc}=14.48$ mA/cm², and FF = 66 %) for **P4**. The addition of porphyrin caused significant increase in J_{sc} and FF values due to balanced charge transport, reduced recombination, favorable blend film morphology, and enhanced crystallinity. The covalent bonding between porphyrin and BODIPY units allowed the control of distance/orientation between donor and acceptor moieties in the polymer backbone. This was claimed to be the key parameter to reach such high-power conversion efficiency in this study.

The early example of *meso*-aryl substituted BODIPY-based donor-acceptor copolymer was based on the report of Chochos *et al.*, in which they developed a novel copolymer **P5** (Figure 10) employing α,β-unsubstituted *meso*-thienyl substituted BODIPY acceptor and dithienovinylene donor.[71] This copolymer showed an ultralow optical band gap of 1.15 eV, and both acceptor and donor units were substituted with linear alkyl chains (—C_8H_{17} and —$C_{12}H_{25}$) to impart solubility in common organic solvents. Furthermore, this semiconductor was the first copolymer based on a α,β-unsubstituted BODIPY π-unit. This copolymer showed a panchromatic absorption profile ranging from 300 nm to 1100 nm, which makes it suitable for near infrared (NIR) organic photovoltaic applications. **P5**:$PC_{71}BM$ blends in different composition ratios were prepared via spin-coating and were studied in inverted BHJ-OPV devices, and the highest performance was obtained with PCE, J_{sc}, V_{oc}, and FF values of 1.10 %, 3.39 mA cm⁻², 0.59 V, and 56.18 %, respectively.

In a very recent study by Sharma et al., a new copolymer **P6** (Figure 10) bearing electron-deficient BODIPY and electron-rich thiophene units linked by ethynyl bridge was synthesized, and its photophysical/electrochemical properties were investigated.[79] Ethynyl bridges were used in the polymeric π-backbone due to its electron-withdrawing nature and the cylindrical-like π-electron density, which leads stabilized HOMO energy level (−5.45 eV). Solution-processed BHJ-OPV devices were fabricated by blending **P6** donor polymer with a carbazole-tetracyanobutadienediketopyrrolo-pyrrole (SMDPP) based non-fullerene acceptor. After the optimization of active layer morphology, very high PCE of 9.29 % was achieved, which is also higher than the devices employing **P6** donor polymer with $PC_{71}BM$ acceptor (7.41 %). This improved power conversion efficiency was attributed to the better light harvesting efficiency

of the **P6:SMDPP** active layer in the near-infrared region, and the higher LUMO energy level of the SMDPP as compared to $PC_{71}BM$. As of the date of this review, this PCE is the highest among all known solar cells based on BODIPY based copolymer.

BODIPYs in Organic Thin-Films Transistors

In addition to photovoltaic applications, BODIPY-based small molecules and polymers have been also explored as electroactive semiconducting materials in TFT devices. However, when compared with BHJ-OPVs, the number of BODIPY semiconductors characterized in OTFTs are much more limited and the device performances are relatively poor with typical charge carrier mobilities of 10^{-2} cm² V^{-1} s⁻¹ or lower. There is only one example of a BODIPY semiconductor showing a charge carrier mobility of > 0.1 cm²V^{-1}s⁻¹.[40] BODIPY π-core possesses a unique electronic structure and its π-architecture has a clear impact on its charge-carrier type.[37,50,125] While π-extension on the BODIPY's *meso*-position leads to *n*-channel semiconducting characteristics,[37] aromatic substitutions at other positions result in *p*-channel transistor behavior.[40] The BODIPY π-core has also been employed as a strong acceptor unit in constructing donor-acceptor (D—A) molecular/polymeric π-architectures, and varied electrical characteristics have been obtained depending on the final molecular structure. Semiconductor thin-films were fabricated via vacuum deposition or solution processing, and not only the electronic feature of the materials, but also the microstructure/morphology of the films have greatly influenced overall charge-transport performance. In this section, we summarize the recent progress (Table 2) in the past decade in BODIPY-based OTFTs focusing on four main material types and investigating the corresponding molecular design, optical and electrochemical characteristics, and device performances along with microstructural/morphological properties.

Semiconductors with a Central BODIPY π-Unit

Note that TFTs based on **9** that has a central BODIPY π-unit was discussed earlier in this review. The only other known examples of molecular semiconductors with a central BODIPY π-unit are **59**–**62**, which were designed and synthesized by Singh *et al.*,
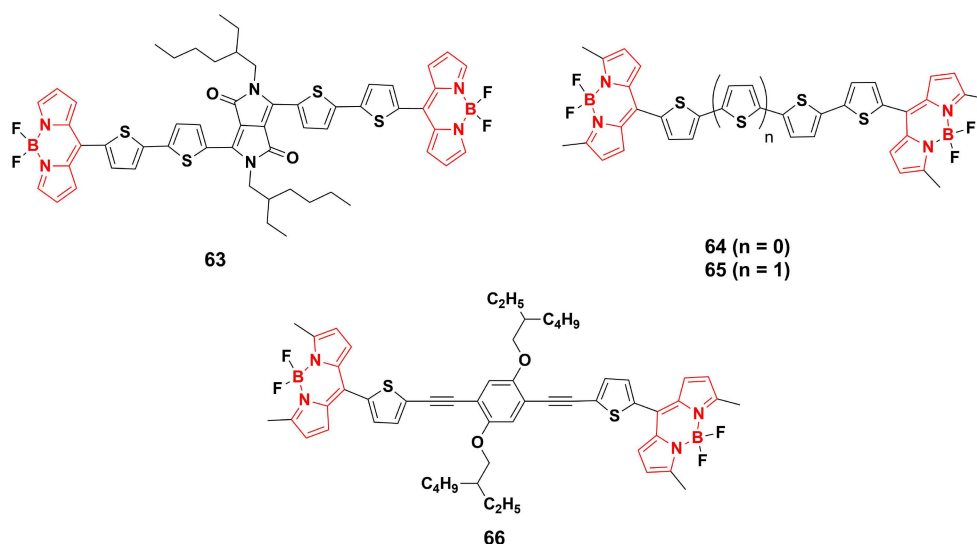
Table 2. Field-effect mobility values, current on/off ratios, and threshold voltages for organic thin-film transistors (OTFTs) employing BODIPY-based semiconductors.

Year	Material	Mobility [cm²V⁻¹s⁻¹]	I_{on}/I_{off}	V_t [V]	Ref.
2011	P5[a]	2.9×10^{-6} (p)	10^3	−75	[39]
	P6[a]	1.6×10^{-9} (p)	10^2	−53	
	P7[a]	3.1×10^{-8} (p)	10^2	−44	
	P8[a]	3.9×10^{-6} (p)	10^3	43	
	P9[a]	1.4×10^{-5} (n)	10^4	37	
2012	9[a]	1.0×10^{-3} (p)	NA	NA	[50]
		1.0×10^{-3} (n)			
2013	P10[a]	2.0×10^{-4} (p)	10^4	−50	[40]
	P11[a]	1.0×10^{-3} (p)	10^5	−32	
	P12[a]	1.7×10^{-1} (p)	10^6	−46	
	P13[a]	7.0×10^{-3} (p)	10^5	−37	
2014	59[a]	8.2×10^{-6} (p)	9.2×10^3	−20	[41]
	60[a]	8.6×10^{-6} (p)	5.3×10^4	−16	
	61[a]	8.7×10^{-6} (p)	3.1×10^4	−20	
	62[a]	1.4×10^{-5} (p)	9.0×10^3	−8.3	
2014	30[a]	3.3×10^{-5} (n)	10^1	7.3	[37]
	31[a]	5.8×10^{-5} (n)	10^2	18	
	32[a]	5.4×10^{-5} (n)	10^2	27	
2015	63[a]	1.5×10^{-5} (p)	–	–	[42]
		2×10^{-6} (n)			
2015	P14[a]	1.0×10^{-2} (p)	4.0×10^3	−9	[43]
	P15[a]	3.2×10^{-6} (p)	8.3×10^3	3	
	P16[a]	8.0×10^{-4} (p)	7.4×10^3	−25	
2016	64[a]	2.7×10^{-4} (p)	9.6×10^5	43	[44]
	65[a]	1.1×10^{-2} (n)	1.5×10^8	19	
2016	P17[a]	6.1×10^{-3} (p)	3.1×10^5	−17	[45]
		3.4×10^{-3} (n)	7.5×10^4	58	
	P18[a]	3.1×10^{-4} (p)	6.9×10^3	−25	
	P19[a]	3.1×10^{-2} (p)	1.3×10^2	−30	
		1.5×10^{-2} (n)	3.0×10^1	40	
2016	P20[a]	7.79×10^{-9} (p)	31.6	−17	[126]
	P21[a]	9.46×10^{-5} (n)	10^4	58	
	P22[a]	5.37×10^{-4} (p)	10^5	−22	
2017	66[a]	4.0×10^{-3} (n)	10^6	–	[127]
2017	67[a]	0.11 (n)	10^6	22.5	[137]
2018	P25[a]	4.9×10^{-4} (p)	10^3	−14	[128]
	P26[a]	4.9×10^{-5} (p)	10^2	−50	

[a] via solution process; NA = not available.

comprising triphenylamine donor end units at 2,6-positions and varying alkyl side chains at *meso*-phenyl group (Figure 11).[41] Homogeneous thin-films were fabricated via solution-processing, and among them, oligoethylene glycol (OEG)-substituted **62** exhibited the highest hole mobility of 1.4×10^{-5} cm²V⁻¹s⁻¹ and threshold voltage of -8.3 V in an OTFT device, which was comparable to regioregular polythiophenes with OEG substituents.[130] It is noteworthy that OEG containing π-conjugated

semiconductors have been rare in the literature, and little attempt has been made to use them in organic (opto) electronics.

Semiconductors with Terminal BODIPY π-units

The semiconductors employing terminal BODIPY π-units were all synthesized with five-membered thiophene units attached to the BODIPY *meso*-positions, and they mainly worked as *n*-type (or ambipolar) organic semiconductors in OTFTs. This particular design was found to show great electronic/structural advantages to enhance charge-transport in the solid state. In the early study, Wang et al. designed and synthesized a novel near-infrared absorbing small molecule **63** (Figure 12) in a conjugated acceptor-donor-acceptor-donor-acceptor (A-D-A-D-A) architecture.[42] Diketopyrrolopyrole (DPP) and BODIPY acceptor building blocks were employed with bithiophene donor bridges. 2-ethylhexl side-chains were added on the central DPP unit to ensure good solubility in organic solvents. This approach was employed to realize strong charge-transfer transition and good π-delocalization.[131] Bottom-contact OTFTs were fabricated, which yielded ambipolar characteristics with moderate hole and electron mobilities of 1.5×10^{-5} cm²V⁻¹s⁻¹ and 2×10^{-6} cm²V⁻¹s⁻¹, respectively. In the same years, Poe et al. investigated the TFT characteristics of **30, 31** and **32**, which were originally developed for use in BHJ-OPVs (Figure 4).[37] Bottom-contact OTFTs were fabricated to examine the charge transport performance of these molecules, and **31** exhibited the highest electron mobility of 5.8×10^{-5} cm²V⁻¹s⁻¹, while **30** exhibited the lowest electron mobility of 3.3×10^{-5} cm²V⁻¹s⁻¹.

Following these two studies, Usta et al. designed and characterized two novel solution-processable BODIPY-based small molecules for OTFTs in a recent study. **64** and **65** were developed based on an acceptor-donor-acceptor molecular system, where BODIPYs were used as terminal acceptors and terthiophene/quaterthiophene were used as the central donor unit (Figure 12).[44] Linear and symmetrical molecular architectures with extended π-conjugations and optimized molecular energetics were achieved by connecting BODIPYs to the α,ω-positions of oligothiophene cores through *meso*-positions. The single-crystal structure of a subunit displayed a relatively planar geometry. The inter-ring torsional angle between the BODIPY plane and the *meso*-thiophene unit was found to be 48.8°, which is smaller than those of the previously reported *meso*-

59: R= Me
60: R=
61: R=
62: R=

59-62

Figure 11. Chemical structures of semiconductors with a central BODIPY π-unit.

63

64 (n = 0)
65 (n = 1)

66

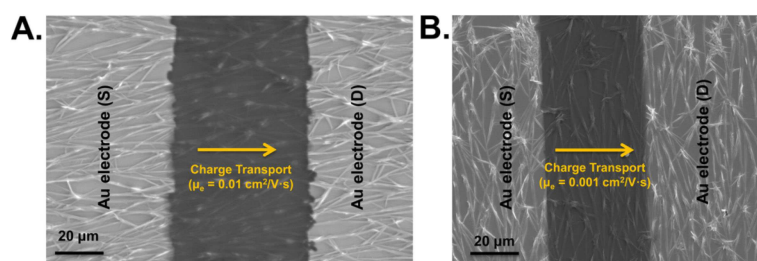**Figure 12.** Chemical structures of semiconductors with terminal BODIPY π-units.

Figure 13. Top-view SEM images of OTFT devices fabricated via solution shearing of **65** with source-drain electrodes deposited perpendicular (A) and parallel (B) to the major fiber alignment direction.[44] Copyright 2016 American Chemical Society. Reproduced with permission from ref. [44].

aromatic substituted BODIPY small molecules (θ = 56–90°). This is ascribed to the absence of β-pyrrole substituents and sterically less hindering nature of the five-membered meso-thiophene ring.[132] The BODIPY core showed slipped cofacial π-stacked packing motif with a beneficial interplanar π–π stacking distance of 3.79–3.97 Å. These structural features offered advantages to enhance charge-transport in the solid state. In addition, the new molecules exhibited unusually good solubilities despite the absense of long lipophilic alkyl substituents. Top-contact/bottom-gate OTFTs were fabricated using solution-sheared films. **65** exhibited an electron mobility of 0.01 cm^{2}V^{-1}s^{-1} with an extremely high I$_{on}$/I$_{off}$ ratio of 10^8, which was higher than those of **64** (2.7 × 10^{-4} cm^{2}V^{-1}s^{-1}). Furthermore, fiber-alignment-induced charge-transport anisotropy (μ$_\parallel$/μ$_\perp$ ≈ 10) was observed, where higher mobilities were achieved for the microfibers along the conduction channel, which enables efficient long-range charge-transport between source and drain electrodes (Figure 13). These OTFT performances were the highest reported for an *n*-type BODIPY-based small molecular semiconductor.

Following their original study on small molecules **64** and **65**, Usta et al. synthesized and characterized another solution-processable acceptor-donor-acceptor (A-D-A) type small molecule, **66**, which consisted of BODIPY end-unit acceptors and a

rod-shaped 1,4-bis-(thienylethynyl)2,5-dialkoxybenzene central donor unit (Figure 12).[127] 2-ethylhexyloxy electron-donating groups were employed on the central phenyl ring. To design a shape-consistent, rod-like structure with an extended π-conjugation length, alkyne linkages were applied between the sterically-bulky central phenyl core and thienyl units.[136] It is known that alkyne linkages are advantageous to assist steric and conformational constraints due to its quasi-cylindrical electronic symmetry. The *meso*-positions of the BODIPYs were used to connect to the thiophene units by minimizing inter-ring torsions between donor and acceptor units. 2-ethylhexyloxy lipophilic substituents were employed for good solubility in common organic solvents. Single-crystal X-ray diffraction (XRD) analysis was employed to reveal crucial structural features and intermolecular interactions of the new semiconductor, and relatively small ''BODIPY-*meso*thiophene'' dihedral angle of 44.94° and antiparallel π-stacked BODIPY dimers with an interplanar distance of 3.93 Å were observed. Solution-shearing method was used to grow highly crystalline one-dimensional (1-D) microribbons on PS (polystyrene)-brush treated substrates (Figure 14). Strong edge-to-face ''C–H(pyrrolic)···π(dialkoxyphenylic) (~2.85 Å)'' with relatively weaker ''π(ethynyl)···π(ethynyl)'' (~4.51 Å) directional interactions were identified to be impactful in the formation of highly crystalline microribbons along the
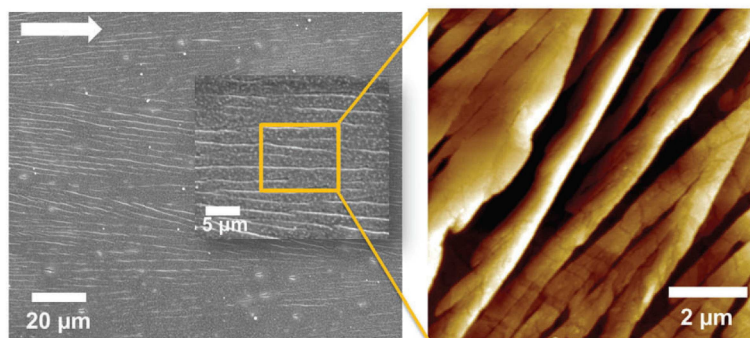
Figure 14. SEM/AFM-topographic images of the solution-sheared **66** thin-film.[127] Copyright 2017 Royal Society of Chemistry. Reproduced with permission from ref. [127].

[100] crystalline direction. Using these microribbons, bottom-gate/top-contact OTFT devices have been fabricated, which exhibited an electron mobility of 4.0×10^{-3} cm^{2}V^{-1}s^{-1} and current on/off ratio of 10^5–10^6. This was the highest electron mobility reported to date for a BODIPY-based small molecular semiconductor with alkyne linkages.

Annulated BODIPY Semiconductors

Although numerous annulated BODIPY-based semiconductors have been reported in BHJ-OPV devices showing appreciable power conversion efficiencies (*vide supra*), to the best of our knowledge, there is only one example of an annulated BODIPY-based semiconductor characterized in TFTs. [137] In this example, **67** (Figure 15) showed an electron mobility of 0.11 cm^{2}V^{-1}s^{-1}

67
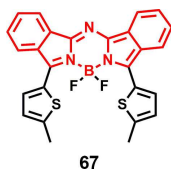
Figure 15. Chemical structures of annulated BODIPY semiconductor **67**.

and I$_{on}$/I$_{off}$ ratio of 10^6. This OTFT device also showed a photoresponse when NIR light was used. We should emphasize that annulated BODIPY-based semiconductors could be a potential research direction for the design, development, and characterization of new BODIPY π-architectures as novel semiconductors in OTFTs.

Copolymers Based on BODIPY π-Acceptor

Copolymers based on BODIPY π-acceptor building blocks have been developed in the past several decades in the literature for various applications, and there are a good number of reports on their OTFT performances. Although they are typically p-type

semiconductors, we should note that there is one study revealing n-type activity (*vide infra*). One of the early studies on BODIPY-based polymeric semiconductors for use in OTFTs was reported by Popere *et al*, in which five novel π-conjugated donor (D) – acceptor (A) type copolymers (**P7-P11**) incorporating BODIPY core along with quinoxaline (Qx), 2,1,3-benzothiadiazole (BzT), N,N'-di(2'-ethyl)hexyl-3,4,7,8-naphthalenetetracarboxylic diimide (NDI), and N,N'-di(2'-ethyl)hexyl-3,4,9,10-perylene tetracarboxylic diimide (PDI) π-acceptors, respectively, were synthesized via Sonogashira cross-coupling polymerizations (Figure 16).[39] In these polymers, while Qx and BzT are *o*-quinoid-type acceptors, NDI and PDI are rylene-type acceptors. Semiconductor layers were spin-coated from 10 mg/mL chlorobenzene solutions onto octadecyltrimethoxysilane (OTS)-treated Si/SiO$_2$ substrates, and bottom-contact thin-film transistors were fabricated. **P7**, **P8**, and **P9** exhibited *p*-type semiconductor behaviors. The highest hole mobility was found to be 2.9×10^{-6} cm^{2}V^{-1}s^{-1} for **P7**. The combination of BzT and Qx in the polymer backbone reduced the mobility of holes by few orders of magnitude. On the other hand, **P10** and **P11** exhibited *n*-type semiconductor behaviors. The electron mobility for **P10** was found to be 3.9×10^{-6} cm^{2}V^{-1}s^{-1}, and, for **P11**, it was an order of magnitude higher (1.4×10^{-5} cm^{2}V^{-1}s^{-1}).

Usta and Facchetti *et al*. developed BODIPY-thiophene copolymers **P12**–**P15** as *p*-channel semiconductor materials for organic thin-film transistors (Figure 16).[40] The planar dipyrromethene π-core unit with effectively delocalized HOMO/LUMO orbitals enabled extended intramolecular π-delocalizations and π–π stackings. The BODIPY units in the copolymers exhibited strong local dipoles ($\mu = 3.38$–4.12 Debye) oriented toward the 4,4'-fluorine substituents, which was found to enhance molecular ordering and thin-film crystallinity via strong dipolar interactions.[122] The alkyl chain of the copolymers at the meso-position and methyl substituents at the α- and β-positions ensured good solution processability and facilitated interdigitation in the solid-state.[129] The polymer thin-films were fabricated via spin-coating and exhibited *p*-type characteristics under ambient conditions. **P12**, **P13**, and **P15** exhibited relatively low hole mobilities of 0.0002–0.007 cm^{2}V^{-1}s^{-1} and current on/off ratios of 10^3–10^5. **P14** exhibited relatively high hole mobility of 0.17 cm^{2}V^{-1}s^{-1} with current on/off ratios of 10^5–10^6. The out-
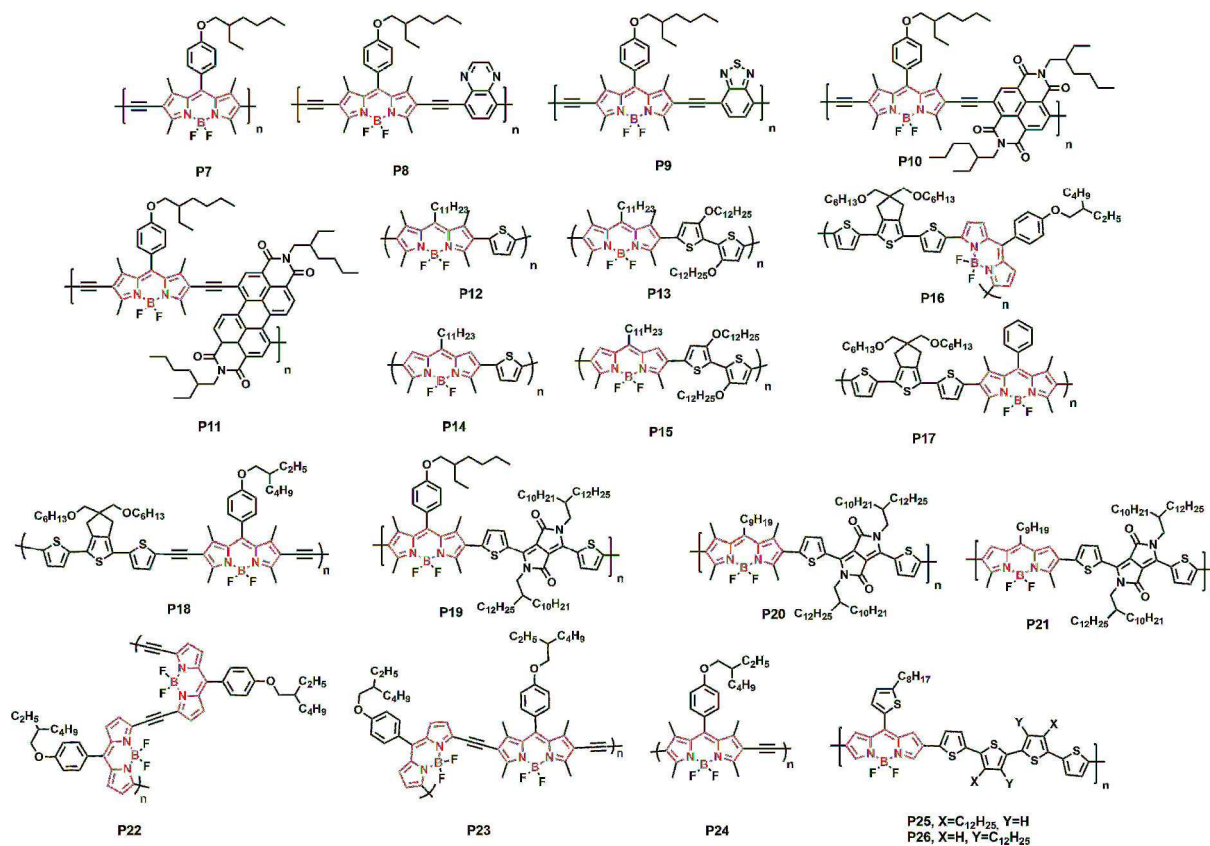
Figure 16. Chemical structures of copolymers based on BODIPY π-acceptor.

standing improvement of mobility in this polymer originated from its favorable film morphology and electronic structure.

Debnath et al. synthesized three new low-band-gap copolymers **P16**–**P18** (Figure 16) by using BODIPY acceptor and thiophene-capped 5,5-bis(hexyloxymethyl)-5,6-dihydro-4H-cyclopenta[c]-thiophene (CPT) donor.[43] The CPT unit was connected through 3,5-positions and 2,6-positions of BODIPY in **P16** and **P17**, respectively, whereas an additional acetylene spacer was used in **P18**. UV-vis-NIR region absorption spectra were recorded to examine the changes in the optical properties of the three polymers. **P16**–**P18** in chloroform solution exhibited absorption maxima (λ_max) at 721, 559, and 631 nm, respectively, and red-shift of 50 nm were observed for thin films. When compared with **P17**, π-conjugation was enhanced in **P18** due to the minimization of the possible steric hindrance by the additional spacer unit. A more red-shifted absorption was observed for **P16** because of the effective conjugation through 3,5-positions of BODIPY. Optical band gaps (E_g^opt) of 1.28, 1.71, and 1.57 eV for **P16**, **P17**, and **P18** respectively, were measured based on the absorption onset, and **P16** showed the lowest band gap for any CPT-containing polymer. Polymer thin-film transistors were fabricated in bottom-contact configuration, and **P16** showed hole mobility of $0.01 \ cm^2 V^{-1} s^{-1}$ in the best device, which was four orders of magnitude higher than that of **P17**. This was the highest reported performance for a BODIPY-based polymer having α-linkages (3,5-positions). This could be attributed to the absence of methyl groups in **P16**, which

enables more effective π-delocalization through α-connections between donor and acceptor units.

Singh et al. designed and synthesized three copolymers (**P19**–**P21** in Figure 16) based on BODIPY and diketopyrrolopyrrole (DPP) building blocks.[45] The band gaps of the polymers were modulated with slight variations in the BODIPY structure. DPP was selected as a comonomer due to its coplanar backbone structure and the presence of quadrupole,[131,134] which facilitates better packing.[134,135] It was noticed that the torsional angle at the connection point between BODIPY and DPP was a function of the methyl units at β, β' positions. **P21** does not have methyl moieties at β, β' positions and exhibited a torsional angle of 27°, which was the lowest among the polymers studied in this work. This matched with the result of vibronic coupling observed in the UV-vis absorption spectrum, which indicated linearity along the polymer backbone. Frontier molecular orbitals, HOMOs and LUMOs, were delocalized along the backbone for all three polymers, indicating ambipolar characteristics. OTFTs were fabricated to examine the electrical performance of polymers. As expected, **P21**, which had the lowest band gap of 1.2 eV among the three polymers, exhibited ambipolar charge transport with the highest hole and electron mobilities of $3.1 \times 10^{-2} \ cm^2 V^{-1} s^{-1}$ and $1.5 \times 10^{-2} \ cm^2 V^{-1} s^{-1}$, respectively.

Debnath and his colleagues synthesized three novel BODIPY-acetylene copolymers **P22**–**P24** using different substitution positions on the BODIPY core (Figure 16).[126] Site selective

polymerization enabled band gap engineering within these copolymers. From **P22** to **P24**, the HOMO energy level significantly changed, while the LUMO level remained very similar. Thin-films were fabricated via spin coating onto octadecyltrimethoxysilane (OTS) modified SiO_2 substrate. Hydrophobic modification of the substrate increased the mobility for **P23** and **P24** by two orders of magnitude while keeping the mobility for **P22** nearly the same. **P22** and **P24** exhibited p-type characteristics with hole mobilities of 7.79×10^{-9} $cm^2 V^{-1} s^{-1}$ and 5.37×10^{-4} $cm^2 V^{-1} s^{-1}$, and current on/off ratios of 10^1–10^5, respectively, while **P23** displayed n-type behavior with an electron mobility of 9.46×10^{-5} $cm^2 V^{-1} s^{-1}$ and current on/off ratio of 10^4. The poor electrical performance of **P22** originated from the backbone curvature in the polymer chain in every monomeric unit, which has a direct effect on thin-film morphology and device performance. This study was the first example of band-gap engineering for BODIPY-acetylene polymeric semiconductors.[126]

In addition to the photovoltaic studies with copolymer **P2** (Figure 8), Usta *et al.* also investigated its OTFT characteristics. The transistor device was fabricated by spin coating copolymer solution on a PS-brush treated substrate, which exhibited a hole mobility of 5×10^{-3} $cm^2 V^{-1} s^{-1}$. The thin-film morphology was studied by XRD and AFM revealing that the formation of lamellar ordering in the out-of-plane crystallographic direction was absent. In the same study, a derivative of **P2** was developed with a thieno[3,2-b]thiophene comonomer, which showed lower performance originating from its much lower molecular weight.[138] More recently, Chochos *et al.* developed two novel ultralow band gap ($E_g < 1.0$ eV) copolymers **P25** and **P26** (Figure 16) based on α,β-unsubstituted *meso*-thienyl substituted BODIPY acceptor and quaterthiophene donor units.[128] The position of the alkyl side chains on the central bithiophene fragment was found to have a direct effect on the optoelectronic and charge transport properties of the final copolymers. Tail-to-tail alkyl chain positioning in **P25** resulted in lower optical band gap and higher charge mobility when compared with the head-to-head alkyl-positioned copolymer **P26**. Both copolymers exhibited p-channel OFET device characteristics in bottom-contact/top-gate device configurations with hole mobilities of 4.7×10^{-4}–10^{-5} $cm^2 V^{-1} s^{-1}$. Despite the low LUMO energy levels for these copolymers (-4.1 eV), the absence of electron-transport was attributed to the poor delocalization of the corresponding LUMOs, the presence of electron traps, and the poor microstructure.

Summary and Outlook

Structural versatility of π-conjugated systems is very crucial to the development of new organic semiconductors, and it allows for the realization of fine-tuned (opto)electronic properties for a particular application. The design and development of novel π-architectures for use in organic semiconductors has always been a key research area in the field of organic (opto) electronics. Since its discovery in the late 1960s, most of the early work on BODIPY-based functional materials has focused

on their synthesis/functionalization and applications in chemosensors, fluorescent switches, and biochemical labelling. Inspired by the great advancements in BHJ-OPVs and OTFTs, BODIPYs have also gained increased attention over the past decade as an effective building block in organic semiconductors.

This review explores the recent progress (2009–2018) in the field of BODIPY-based organic semiconductors that have been characterized in BHJ-OPVs and OTFTs. The structural and (opto) electronic properties, as well as their device performances with microstructural and morphological properties are deeply studied in this review, and the corresponding device performances are summarized in Tables 1 and 2. Despite low charge carrier mobilities ($\sim 10^{-5}$–10^{-3} $cm^2 V^{-1} s^{-1}$) and poor photovoltaic performances (PCEs ~ 1–2%) reported only a decade ago, promising results with carrier mobilities of ~ 0.01–0.2 $cm^2 V^{-1} s^{-1}$ and PCEs of ~ 6–9% were achieved in OTFTs and OPVs with recently developed BODIPY π-architectures. In fact, the most promising results to this end were mostly achieved in the past 2–3 years. Although the research on BODIPY-based molecules is still at its early stage with regards to realizing high performances, BODIPY moieties have already demonstrated great potential rendering them a promising class of materials for further opportunities in (opto)electronic technologies. Although BODIPY offers numerous advantageous electronic and structural features as discussed in this review, its most unique properties, which certainly differentiate BODIPY from the other π-systems, are its very high molecular dipole moment and that it could enable good solubility in common organic solvents without the need for long lipophilic alkyl substituents. We believe that these features, along with others, can vastly expand the applicability of BODIPYs to the field of high-performance BHJ-OPVs and OTFTs. In our opinion, continued synthesis and device studies on BODIPY-based semiconductors are quite essential not only to increase current device performances and open new opportunities, but also to establish a strong understanding of material structure–property–optoelectronic performance relationships. Based on the performance values obtained in these studies reviewed here, it could be suggested that BODIPY-based conjugated systems have a high potential for further development and represent a remarkable platform for the molecular engineering of solution-processable electro-active materials in organic (opto)electronics.

Conflict of Interest

The authors declare no conflict of interest.

[1] H. Shirakawa, J. Louis, A. G. Macdiarmid, *J. C. S. Chem. Comm.* **1977**, 578–580.

[2] K. A. Mazzio, C. K. Luscombe, *Chem. Soc. Rev.* **2015**, *44*, 78–90.

[3] J. Lee, H. F. Chen, T. Batagoda, C. Coburn, P. I. Djurovich, M. E. Thompson, S. R. Forrest, *Nat. Mater.* **2016**, *15*, 92–98.

[4] W. J. Hyun, E. B. Secor, M. C. Hersam, C. D. Frisbie, L. F. Francis, *Adv. Mater.* **2015**, *27*, 109–115.

[5] B. Lussem, C.-M. Keum, D. Kasemann, B. Naab, Z. Bao, K. Leo, *Chem. Rev.* **2016**, *116*, 13714–13751.

[6] M. Braendlein, A.-M. Pappa, M. Ferro, A. Lopresti, C. Acquaviva, E. Mamessier, G. G. Malliaras, R. M. Owens, *Adv. Mater.* **2017**, *29*, 1605744.

[7] T. Erdmann, S. Fabiano, B. Milián-Medina, D. Hanifi, Z. Chen, M. Berggren, J. Gierschner, A. Salleo, A. Kiriy, B. Voit, A. Facchetti, *Adv. Mater.* **2016**, *28*, 9169–9174.

[8] J. L. Marshall, K. Uchida, C. K. Frederickson, C. Schutt, A. M. Zeidell, K. P. Goetz, T. W. Finn, K. Jarolimek, L. N. Zakharov, C. Risko, R. Herges, O. D. Jurchescu, M. M. Haley, *Chem. Sci.* **2016**, *7*, 5547–5558.

[9] S. Lee, A. Reuveny, J. Reeder, S. Lee, H. Kin, Q. Liu, T. Yokota, T. Sekitani, T. Isoyama, Y. Abe, Z. Suo, T. Someya, *Nat. Nanotechnol.* **2016**, *11*, 472–478.

[10] C. Zhang, P. Chen, W. Hu, *Small* **2016**, *10*, 1252–1294.

[11] C. Di, F. Zhang, D. Zhu, *Adv. Mater.* **2013**, *25*, 313–330.

[12] H. Chen, M. Hurhangee, M. Nikolka, W. Zhang, M. Kirkus, M. Neophytou, S. J. Cryer, D. Harkin, P. Hayoz, M. Abdi-Jalebi, C. R. McNeill, H. Sirringhaus, I. McCulloch, *Adv. Mater.* **2017**, *29*, 1702523.

[13] M. Stolte, S.-L. Suraru, P. Diemer, T. He, C. Burschka, U. Zschieschang, H. Klauk, F. Wurthner, *Adv. Funct. Mater.* **2016**, *26*, 7415–7422.

[14] M. Schwarze, W. Tress, B. Beyer, F. Gao, R. Scholz, C. Poelking, K. Ortstein, A. A. Gunther, D. Kasemann, D. Andrienko, K. Leo, *Science* **2016**, *352*, 1446–1449.

[15] D. Ho, M. Jeon, H. Kim, O. Gidron, C. Kim, S. Y. Seo, *Org. Electron.* **2018**, *52*, 356–363.

[16] M. R. Reddy, H. Kim, C. Kim, S. Y. Seo, *Synth. Met.* **2018**, *235*, 153–159.

[17] N. C. Mamillapalli, S. Vegiraju, P. Priyanka, C.-Y. Lin, X.-L. Luo, H.-C. Tsai, S.-H. Hong, J.-S. Ni, W.-C. Lien, G. Kwon, S. L. Yau, C. Kim, C.-L. Liu, M.-C. Chen, *Dyes Pigm.* **2017**, *145*, 584–590.

[18] R. Ozdemir, D. Choi, M. Ozdemir, G. Kwon, H. Kim, U. Sen, C. Kim, H. Usta, *J. Mater. Chem. C* **2017**, *5*, 2368–2379.

[19] X. Y. Chin, G. Pace, C. Soci, M. Caironi, *J. Mater. Chem. C* **2017**, *5*, 754–762.

[20] W. Zhang, Y. Han, X. Zhu, Z. Fei, Y. Feng, N. D. Treat, H. Faber, N. Stingelin, I. McCulloch, T. D. Anthopoulos, M. Heeney, *Adv. Mater.* **2016**, *28*, 3922–3927.

[21] C. Mitsui, H. Tsuyama, R. Shikata, Y. Murata, H. Kuniyasu, M. Yamagishi, H. Ishii, A. Yamamoto, Y. Hirose, M. Yano, T. Takehara, T. Suzuki, H. Sato, A. Yamano, E. Fukuzaki, T. Watanabe, Y. Usami, J. Takeya, T. Okamoto, *J. Mater. Chem. C* **2017**, *5*, 1903–1909.

[22] K. Yoshikawa, H. Kawasaki, W. Yoshida, T. Irie, K. Konishi, K. Nakano, T. Uto, D. Adachi, M. Kanematsu, H. Uzu, K. Yamamoto, *Nat. Energy* **2017**, *2*, 17032.

[23] T. Kim, J.-H. Kim, T. E. Kang, C. Lee, H. Kang, M. Shin, C. Wang, B. Ma, U. Jeong, T.-S. Kim, B. J. Kim, *Nat. Commun.* **2015**, *6*, 8547.

[24] S.-S. Cheng, P.-Y. Huang, M. Ramesh, H.-C. Chang, L.-M. Chen, C.-M. Yeh, C.-L. Fung, M.-C. Wu, C.-C. Liu, C. Kim, H.-C. Lin, M.-C. Chen, C.-W. Chu, *Adv. Funct. Mater.* **2014**, *24*, 2057.

[25] K. M. Boopathi, R. Mohan, T.-Y. Huang, W. Budiawan, M.-Y. Lin, C.-H. Lee, K.-C. Ho, C.-W. Chu, *J. Mater. Chem. A* **2016**, *4*, 1591–1597.

[26] A. Melianas, V. Pranculis, Y. Xia, N. Felekidis, O. Inganas, V. Gulbinas, M. Kemerink, *Adv. Energy Mater.* **2017**, *7*, 1602143.

[27] S. Mukherjee, C. M. Proctor, J. R. Tumbleston, G. C. Bazan, T.-Q. Nguyen, H. Ade, *Adv. Mater.* **2015**, *27*, 1105–1111.

[28] N. Zhou, K. Prabakaran, B. Lee, S. H. Chang, B. Harutyunyan, P. Guo, M. R. Butler, A. Timalsina, M. J. Bedzyk, M. A. Ratner, S. Vegiraju, S. Yau, C.-G. Wu, R. P. H. Chang, A. Facchetti, M.-C. Chen, T. J. Marks, *J. Am. Chem. Soc.* **2015**, *137*, 4414–4423.

[29] N. Zhou, S. Vegiraju, X. Yu, E. F. Manley, M. R. Butler, M. J. Leonardi, P. Guo, W. Zhao, Y. Hu, K. Prabakaran, R. P. H. Chang, M. A. Ratner, L. X. Chen, A. Facchetti, M.-C. Chen, T. J. Marks, *J. Mater. Chem. C* **2015**, *3*, 8932–8941.

[30] T. Ma, K. Jiang, S. Chen, H. Hu, H. Lin, Z. Li, J. Zhao, Y. Liu, Y.-M. Chang, C.-C. Hsiao, H. Yan, *Adv. Energy Mater.* **2015**, *5*, 1501282.

[31] A. Treibs, F.-H. Kreuzer, *Justus Liebigs Ann. Chem.* **1968**, *718*, 208–223.

[32] T. Kowada, H. Maeda, K. Kikuchi, *Chem. Soc. Rev.* **2015**, *44*, 4953.

[33] A. Zampetti, A. Minotto, B. M. Squeo, V. G. Gregoriou, S. Allard, U. Scherf, C. L. Chochos, F. Cacialli, *Sci. Rep.* **2017**, *7*, 1611.

[34] M. Chapran, E. Angioni, N. J. Findlay, B. Breig, V. Cherpak, P. Stakhira, T. Tuttle, D. Volyniuk, J. V. Grazulevicius, Y. A. Nastishin, O. D. Lavrentovich, P. J. Skabara, *ACS Appl. Mater. Interfaces* **2017**, *9*, 4750–4757.

[35] N. Boens, V. Leen, W. Dehaen, *Chem. Soc. Rev.* **2012**, *41*, 1130–1172.

[36] N. Boens, B. Verbelen, W. Dehaen, *Eur. J. Org. Chem.* **2015**, 6577–6595.

[37] A. M. Poe, A. M. Della Pelle, A. V. Subrahmanyam, W. White, G. Wantz, S. Thayumanavan, *Chem. Commun.* **2014**, *50*, 2913–2915.

[38] M. Ozdemir, S. W. Kim, H. Kim, M.-G. Kim, B. J. Kim, C. Kim, H. Usta, *Adv. Electron. Mater.* **2018**, *4*, 1700354.

[39] B. C. Popere, A. M. Della Pelle, S. Thayumanavan, *Macromolecules* **2011**, *44*, 4767–4776.

[40] H. Usta, M. D. Yilmaz, A.-J. Avestro, D. Boudinet, M. Denti, W. Zhao, J. F. Stoddart, A. Facchetti, *Adv. Mater.* **2013**, *25*, 4327–4334.

[41] S. Singh, V. Venugopalan, K. Krishnamoorthy, *Phys. Chem. Chem. Phys.* **2014**, *16*, 1337–13382.

[42] Y. Wang, J. Chen, Y. Zhen, H. Jiang, G. Yu, Y. Liu, E. Baranoff, H. Tan, W. Zhu, *Mater. Lett.* **2015**, *139*, 130–133.

[43] S. Debnath, S. Singh, A. Bedi, K. Krishnamoorthy, S. S. Zade, *J. Phys. Chem. C* **2015**, *119*, 15859–15867.

[44] M. Ozdemir, D. Choi, G. Kwon, Y. Zorlu, B. Cosut, H. Kim, A. Facchetti, C. Kim, H. Usta, *ACS Appl. Mater. Interfaces* **2016**, *8*, 14077–14087.

[45] S. Singh, S. Chithiravel, K. Krishnamoorthy, *J. Phys. Chem. C* **2016**, *120*, 26199–26205.

[46] T. Rousseau, A. Cravino, T. Bura, G. Ulrich, R. Ziessel, J. Roncali, *Chem. Commun.* **2009**, *0*, 1673–1675.

[47] T. Rousseau, A. Cravino, T. Bura, G. Ulrich, R. Ziessel, J. Roncali, *J. Mater. Chem.* **2009**, *19*, 2298–2300.

[48] H.-Y. Lin, W.-C. Huang, Y.-C. Chen, H.-H. Chou, C.-Y. Hsu, J. T. Lin, H.-W. Lin, *Chem. Commun.* **2012**, *48*, 8913–8915.

[49] Y. Hayashi, N. Obata, M. Tamaru, S. Yamaguchi, Y. Matsuo, A. Saeki, S. Seki, Y. Kureishi, S. Saito, S. Yamaguchi, H. Shinokubo, *Org. Lett.* **2012**, *14*, 866–869.

[50] T. Bura, N. Leclerc, S. Fall, P. Léveque, T. Heiser, P. Retailleau, S. Rihn, A. Mirloup, R. Ziessel, *J. Am. Chem. Soc.* **2012**, *134*, 17404–17407.

[51] A. Mirloup, N. Leclerc, S. Rihn, T. Bura, R. Bechara, A. Hebraud, P. Leveque, T. Heiser, R. Ziessel, *New J. Chem.* **2014**, *38*, 3644–3653.

[52] S. Kolemen, Y. Cakmak, T. Ozdemir, S. Erten-Ela, M. Buyuktemiz, Y. Dede, E. U. Akkaya, *Tetrahedron* **2014**, *70*, 6229–6234.

[53] W. Liu, A. Tang, J. Chen, Y. Wu, C. Zhan, J. Yao, *ACS Appl. Mater. Interfaces* **2014**, *6*, 22496–22505.

[54] A. Sutter, P. Retailleau, W.-C. Huang, H.-W. Lin, R. Ziessel, *New J. Chem.* **2014**, *38*, 1701–1710.

[55] W. He, Y. Jiang, Y. Qin, *Polym. Chem.* **2014**, *5*, 1298–1304.

[56] A. F. Paterson, S. Singh, K. J. Fallon, T. Hodsden, Y. Han, B. C. Schroeder, H. Bronstein, M. Heeney, I. McCulloch, T. D. Anthopoulos, *Adv. Mater.* **2018**, 1801079.

[57] H. Lee, C. Park, D. H. Sin, J. H. Park, K. Cho, *Adv. Mater.* **2018**, 1800453.

[58] B. Walker, C. Kim, T. Q. Nguyen, *Chem. Mater.* **2010**, *23*, 470–482.

[59] Y. Sun, G. C. Welch, W. L. Leong, C. J. Takacs, G. C. Bazan, A. J. Heeger, *Nat. Mater.* **2012**, *11*, 44–48.

[60] Y. Lin, Y. Fan, Y. Li, X. Zhan, *Adv. Mater.* **2012**, *24*, 3087–3106.

[61] S. Qu, H. Tian, *Chem. Commun.* **2012**, *48*, 3039–3051.

[62] P. Kumaresan, S. Vegiraju, Y. Ezhumalai, S. L. Yau, C. Kim, W.-H. Lee, M.-C. Chen, *Polymer* **2014**, *6*, 2645–2669.

[63] T. Rousseau, A. Cravino, E. Ripaud, P. Leriche, S. Rihn, A. De Nicola, R. Ziessel, J. Roncali, *Chem. Commun.* **2010**, *46*, 5082–5084.

[64] J. Meiss, F. Holzmueller, R. Gresser, K. Leo, M. Riede, *Appl. Phys. Lett.* **2011**, *99*, 193307.

[65] Y. Kubo, K. Watanabe, R. Nishiyabu, R. Hata, A. Murakami, T. Shoda, H. Ota, *Org. Lett.* **2011**, *13*, 4574–4577.

[66] J. J. Chen, S. M. Conron, P. Erwin, M. Dimitriou, K. McAlahney, M. E. Thompson, *ACS Appl. Mater. Interfaces* **2015**, *7*, 662–669.

[67] S. Kraner, J. Widmer, J. Benduhn, E. Hieckmann, T. Jageler-Hoheisel, S. Ullbrich, D. Schutze, K. S. Radke, G. Cuniberti, F. Ortmann, M. Lorenz-Rothe, R. Meerheim, D. Spoltore, K. Vandewal, C. Koerner, K. Leo, *Phys. Status Solidi A* **2015**, *212*, 2747–2753.

[68] W. Liu, J. Yao, C. Zhan, *RSC Adv.* **2015**, *5*, 74238–74241.

[69] J. Liao, Y. Xu, H. Zhao, Y. Wang, W. Zhang, F. Peng, S. Xie, X. Yang, *RSC Adv.* **2015**, *5*, 86453–86462.

[70] L. Xiao, H. Wang, K. Gao, L. Li, C. Liu, X. Peng, W.-Y. Wong, W.-K. Wong, X. Zhu, *Chem. Asian J.* **2015**, *10*, 1513–1518.

[71] B. M. Squeo, N. Gasparini, T. Ameri, A. Palma-Cando, S. Allard, V. G. Gregoriou, C. J. Brabec, U. Scherf, C. L. Chochos, *J. Mater. Chem. A* **2015**, *3*, 16279–16286.

[72] M. L. Rothe, K. S. Schellhammer, T. J. Hoheisel, R. Meerheim, S. Kraner, M. P. Hein, C. Schünemann, M. L. Tietze, M. Hummert, F. Ortmann, G. Cuniberti, C. Körner, K. Leo, *Adv. Electron. Mater.* **2016**, 1600152.

[73] R. S. Rao, A. Bagui, G. H. Rao, V. Gupta, S. P. Singh, *Chem. Commun.* **2017**, *53*, 6953–6956.

[74] I. Bulut, Q. Huaulme, A. Mirloup, P. Chavez, S. Fall, A. Hebraud, S. Mery, B. Heinrich, T. Heiser, P. Leveque, N. Leclerc, *ChemSusChem* **2017**, *10*, 1878–1882.

[75] J. Liao, Y. Xu, H. Zhao, Q. Zong, Y. Fang, *Org. Electron.* **2017**, *49*, 321–333.

[76] T. Y. Li, T. Meyer, R. Meerheim, M. Hoppner, C. Korner, K. Vandewal, O. Zeika, K. Leo, *J. Mater. Chem. A* **2017**, *5*, 10696–10703.

[77] L. Bucher, N. Desbois, P. D. Harvey, C. P. Gros, G. D. Sharma, *ACS Appl. Mater. Interfaces* **2018**, *10*, 992–1004.

[78] L. Bucher, N. Desbois, E. N. Koukaras, C. H. Devillers, S. Biswas, G. D. Sharma, C. P. Gros, *J. Mater. Chem. A* **2018**, *6*, 8449–8461.

[79] L. Bucher, N. Desbois, P. D. Harvey, C. P. Gros, R. Misra, G. D. Sharma, *ACS Appl. Energy Mater.* **2018**, *1*, 3359–3368.

[80] C. J. Brabec, A. Cravino, D. Meissner, N. S. Sariciftci, T. Fromhertz, M. T. Rispens, L. Sanchess, J. C. Hummelen, *Adv. Funct. Mater.* **2001**, *11*, 374.

[81] A. Gadisa, M. Svensson, M. R. Andersson, O. Inganas, *Appl. Phys. Lett.* **2004**, *84*, 1609.

[82] N. Sakai, J. Mareda, E. Vauthey, S. Mable, *Chem. Commun.* **2010**, *46*, 4225.

[83] R. Gresser, M. Hummert, H. Hartmann, K. Leo, M. Riede, *Chem. Eur. J.* **2011**, *17*, 2939.

[84] Y. Kubo, Y. Minowa, T. Shoda, K. Takeshita, *Tetrahedron Lett.* **2010**, *51*, 1600–1602.

[85] H. Kim, A. Burghart, M. B. Welch, J. Reibenspies, K. Burgess, *Chem. Commun.* **1999**, 1889–1890.

[86] A. Loudet, R. Bandichhor, K. Burgess, A. Palma, S. O. McDonnell, M. J. Hall, D. F. O'Shea, *Org. Lett.* **2008**, *10*, 4771–4774.

[87] Y. He, G. Zhao, B. Peng, Y. Li, *Adv. Funct. Mater.* **2010**, *20*, 3383–3389.

[88] D. W. Sievers, V. Shrotriya, Y. Yang, *J. Appl. Phys.* **2006**, *100*, 114509.

[89] J. E. Anthony, J. S. Brooks, D. L. Eaton, S. R. Parkin, *J. Am. Chem. Soc.* **2001**, *123*, 9482.

[90] M. T. Lloyd, A. C. Mayer, S. Subramanian, D. A. Mourey, D. J. Herman, A. V. Bapat, J. E. Anthony, G. G. Malliaras, *J. Am. Chem. Soc.* **2007**, *129*, 9144.

[91] K. N. Winzenberg, P. Kemppinen, G. Fanchini, M. Bown, G. E. Collis, C. M. Forsyth, K. Hegedus, T. B. Singh, S. E. Watkins, *Chem. Mater.* **2009**, *21*, 5701.

[92] S. Ito, T. Murashima, N. Ono, H. Uno, *Chem. Commun.* **1998**, 1661–1662.

[93] S. Aramaki, Y. Sakai, N. Ono, *Appl. Phys. Lett.* **2004**, *84*, 2085.

[94] Y. Matsuo, Y. Sato, T. Niinomi, I. Soga, H. Tanaka, E. Nakamura, *J. Am. Chem. Soc.* **2009**, *131*, 16048.

[95] T. Y. Chu, J. Lu, S. Beaupre, Y. Zhang, J. R. Pouliot, J. Zhou, A. Najari, M. Leclerc, Y. Tao, *Adv. Funct. Mater.* **2012**, *22*, 2345–2351.

[96] W. Shockley, H. J. Queisser, *J. Appl. Phys.* **1961**, *32*, 510–519.

[97] A. Burghart, H. J. Kim, M. B. Welch, L. H. Thorensen, J. Reibenspies, K. Burgess, F. Bergstrom, L. B. A. Johansson, *J. Org. Chem.* **1999**, *64*, 7813–7819.

[98] S. Kolemen, O. A. Bozdemir, Y. Cakmak, G. Barin, S. Erten-Ela, M. Marszalek, J.-H. Yum, S. M. Zakeeruddin, M. K. Nazeeruddin, M. Gratzel, E. U. Akkaya, *Chem. Sci.* **2011**, *2*, 949–954.

[99] B. Jiang, X. Zhang, C. Zhan, Z. Lu, J. Huang, X. Ding, S. He, J. Yao, *Polym. Chem.* **2013**, *4*, 4631–4638.

[100] J. C. Forgie, P. J. Skabara, I. Stibor, F. Vilela, Z. Vobecka, *Chem. Mater.* **2009**, *21*, 1784–1786.

[101] B. C. Popere, A. M. Della Pelle, A. Poe, G. Balaji, S. Thayumanavan, *Chem. Sci.* **2012**, *3*, 3093–3102.

[102] E. H. A. Beckers, P. A. van Hal, A. Dhanabalan, S. C. J. Meskers, J. Knol, J. C. Hummelen, R. A. J. Janssen, *J. Phys. Chem. A* **2003**, *107*, 6218–6224.

[103] M. T. Dang, L. Hirsch, G. Wantz, *Adv. Mater.* **2011**, *23*, 3597–3602.

[104] J. Peet, A. J. Heeger, G. C. Bazan, *Acc. Chem. Res.* **2009**, *42*, 1700–1708.

[105] A. Facchetti, *Chem. Mater.* **2011**, *23*, 733–758.

[106] J. A. G. Williams, *Top. Curr. Chem.* **2007**, *281*, 205–268.

[107] W.-Y. Wong, *Dalton Trans.* **2007**, *0*, 4495–4510.

[108] L. Y. Yan, Y. Zhao, X. Wang, X.-Z. Wang, W.-Y. Wong, Y. Liu, W. Wu, Q. Xiao, G. Wang, X. Zhou, W. Zeng, C. Li, X. Wang, H. Wu, *Macromol. Rapid Commun.* **2012**, *33*, 603–609.

[109] J. S. Wilson, A. Kohler, R. H. Friend, M. K. Al-Suti, M. R. A. Al-Mandhary, M. S. Khan, P. R. Raithby, *J. Chem. Phys.* **2000**, *113*, 7627.

[110] Y. Liu, S. Jiang, K. Glusac, D. H. Powell, D. F. Anderson, K. S. Schanze, *J. Am. Chem. Soc.* **2002**, *124*, 12412–12413.

[111] G. Ramakrishna, T. Goodson III, J. E. Rogers-Haley, T. M. Cooper, D. G. McLean, A. Urbas, *J. Phys. Chem. C* **2009**, *113*, 1060–1066.

[112] X. Qi, ; N. Li, S. R. Forrest, *J. Appl. Phys.* **2010**, *107*, 014514; N. Li, S. R. Forrest, *J. Appl. Phys.* **2010**, *107*, 014514.

[113] V. Steinmann, N. M. Kronenberg, M. R. Lenze, S. M. Graf, D. Hertel, K. Meerholz, H. Burckstummer, E. V. Tulyakova, F. Wurthner, *Adv. Energy Mater.* **2011**, *1*, 888–893.

[114] Y. Sun, J. H. Seo, C. J. Takacs, J. Seifter, A. J. Heeger, *Adv. Mater.* **2011**, *23*, 1679–1683.

[115] R. Gresser, M. Hummert, H. Hartmann, K. Leo, M. Riede, *Chem. Eur. J.* **2011**, *17*, 2939–2947.

[116] L. J. Huo, S. Q. Zhang, X. Guo, F. Xu, Y. F. Li, J. H. Hou, *Angew. Chem.* **2011**, *123*, 9871–9876; *Angew. Chem. Int. Ed.* **2011**, *50*, 9697–9702.

[117] J. C. Bijleveld, R. A. M. Verstrijden, M. M. Wienk, R. A. J. Janssen, *J. Mater. Chem.* **2011**, *21*, 9224–9231.

[118] S. Inagi, K. Naka, Y. Chujo, *J. Polym. Sci. A Polym. Chem.* **2007**, *45*, 3770–3775.

[119] O. Aleveque, P. Leriche, N. Cocherel, P. Frere, A. Cravino, J. Roncali, *Sol. Energ. Mat. Sol.* **2008**, *92*, 1170–1174.

[120] I. Bulut, P. Chavez, A. Mirloup, Q. Huaulme, B. Heinrich, A. Hebraud, S. Mery, R. Ziessel, T. Heiser, P. Leveque, N. Leclerc, *J. Mater. Chem. C* **2016**, *4*, 4296–4303.

[121] I. Bulut, P. Leveque, B. Heinrich, T. Heiser, R. Bechara, N. Zimmermann, S. Mery, R. Ziessel, N. Leclerc, *J. Mater. Chem. A* **2015**, *3*, 6620–6628.

[122] J. A. Letizia, M. R. Salata, C. M. Tribout, A. Facchetti, M. A. Ratner, T. J. Marks, *J. Am. Chem. Soc.* **2008**, *130*, 9679–9694.

[123] G. Ren, E. Ahmed, S. A. Jenekhe, *Adv. Energy Mater.* **2011**, *1*, 946–953.

[124] P. Cheng, L. Ye, X. Zhao, J. Hou, Y. Li, X. Zhan, *Energy Environ. Sci.* **2014**, *7*, 1351–1356.

[125] B. M. Squeo, V. G. Gregoriou, A. Avgeropoulos, S. Baysec, S. Allard, U. Scherf, C. L. Chochos, *Prog. Polym. Sci.* **2017**, *71*, 26–52.

[126] S. Debnath, S. Singh, A. Bedi, K. Krishnamoorthy, S. S. Zade, *J. Polym. Sci. Part A* **2016**, *54*, 1978–1986.

[127] M. Ozdemir, D. Choi, Y. Zorlu, B. Cosut, H. Kim, C. Kim, H. Usta, *New J. Chem.* **2017**, *41*, 6232–6240.

[128] B. M. Squeo, V. G. Gregoriou, Y. Han, A. Palma-Cando, S. Allard, E. Serpetzoglou, I. Konidakis, E. Stratakis, A. Avgeropoulos, T. D. Anthopoulos, M. Heeney, U. Scherf, C. L. Chochos, *J. Mater. Chem. C* **2018**, *6*, 4030–4040.

[129] S. Grunder, C. Valente, A. C. Whalley, S. Sampath, J. Portmann, Y. Y. Botros, J. F. Stoddart, *Chem. Eur. J.* **2012**, *18*, 15632–15649.

[130] M. Shao, Y. He, K. Hong, C. M. Rouleau, D. B. Geohegan, K. Xiao, *Polym. Chem.* **2013**, *4*, 5270–5274.

[131] C. B. Nielsen, M. Turbiez, I. McCulloch, *Adv. Mater.* **2013**, *25*, 1859–1880.

[132] Y. Yang, Q. Guo, H. Chen, Z. Zhou, Z. Guo, Z. Shen, *Chem. Commun.* **2013**, *49*, 3940–3942.

[133] D. Khim, Y. R. Cheon, Y. Xu, W.-T. Park, S.-K. Kwon, Y.-Y. Noh, Y.-H. Kim, *Chem. Mater.* **2016**, *28*, 2287–2294.

[134] A. L. Kanibolotsky, F. Vilela, J. C. Forgie, S. E. Elmasly, P. J. Skabara, K. Zhang, B. Tieke, J. McGurk, C. R. Belton, P. N. Stavrinou, D. D. Bradley, *Adv. Mater.* **2011**, *23*, 2093–2097.

[135] M. Gsanger, D. Bialas, L. Huang, M. Stolte, F. Wurthner, *Adv. Mater.* **2016**, *28*, 3615–3645.

[136] F. Silvestri, A. Marrocchi, M. Seri, C. Kim, T. J. Marks, A. Facchetti, A. Taticchi, *J. Am. Chem. Soc.* **2010**, *132*, 6108–6123.

[137] F. Li, Y. Chen, C. Ma, U. Buttner, K. Leo, T. Wu, *Adv. Electron. Mater.* **2017**, *3*, 1600430.

[138] R. J. Kline, M. D. McGehee, E. N. Kadnikova, J. Liu, J. M. J. Frechet, M. F. Toney, *Macromolecules* **2005**, *38*, 3312–3319.